Tetrahedral and Other M_2L_6 Transition Metal Dimers

Richard H. Summerville and Roald Hoffmann*

Contribution from the Department of Chemistry and Materials Science Center, Cornell University, Ithaca, New York 14853. Received March 3, 1976

Abstract: This theoretical study shows how three factors influence the geometry and electronic structure of dimeric tetrahedral and square planar transition metal complexes of the M_2L_6 type. The factors are (1) the geometrical preference of the monomer, (2) the symmetry-restricted opportunities for coupling through the orbitals of the bridging groups, (3) direct metal–metal overlap. In analyzing the first factor, we find that in tetrahedral d^{10} monomers of the MX_2Y_2 type, the angle between the better π acceptors and better σ donors should be opened up. The structures of monomeric dinitrosyls are rationalized, including the minor deviations from MNO linearity. Superposition of the calculated MX_2Y_2 monomer structures into a $X_2MY_2MX_2$ dimer gives a reference point relative to which elongation or contraction of the bridge region as a consequence of through-bond coupling or metal–metal bonding can be evaluated. In the tetrahedral d^9 dimers we find little direct metal–metal σ bonding, in the d^8 dimers a strong metal–metal π bond. Locally square planar dimers are studied, with an emphasis on the interconversion of the alternate square planar and tetrahedral geometries. The orbitals of the bridging group are determinative here, with π-donors favoring the square planar extreme. The simple twist interconverting the two structures is symmetry forbidden. We study the hinging distortion in the square planar dimers, failing to find a controlling electronic effect for this soft surface. Other geometries, such as the directly metal–metal bridged $Ni_2(CN)_6^{4-}$ type, are also examined.

The thesis of a series of theoretical investigations, of which this is the first contribution, is that there are three determinants of the geometrical and electronic structure of bridged metal dimer complexes: (1) the geometrical preference of the monomer fragment; (2) the opportunity for interaction offered up by the orbitals of the bridging groups—a factor we have called in another context "through-bond coupling";[1] (3) direct bonding or antibonding overlap of primarily metal-centered orbitals. The mix of these contributions is variable and rarely does a single one dominate.

There is little novel in the recognition of these individual factors. To cite a few among many relevant previous studies, we point first of all to the elegant and far-reaching work of Dahl and collaborators[2] recently buttressed by theoretical studies of the Fenske group, on all aspects of metal–metal bonding but especially on the structural consequences thereof; to the contribution of Cotton, who incisively analyzed the entire range of structural deformations in confacial octahedral dimers with respect to an ideal face-sharing structure[3]; and to the work of Mason and Mingos on the role of bridging group orbitals on metal–metal distances.[4] These and other workers[5] have noted that direct metal–metal overlap may not be the sole cause of either a low-spin ground state or a short metal–metal separation. We view as our minor contribution the systematic theoretical analysis of all three factors in the context of the available structural information. This first paper deals primarily with "tetrahedral" metal dimer complexes of the general type **1**.


1
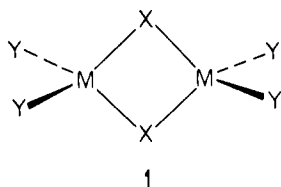
Subsequent contributions will discuss triply bridging "octahedral" dimers, other less symmetrical structures, and polynuclear chains, while a previously published paper has analyzed weakly coupled systems of the Cu(II) dimer type.[1b]

Structural Features of Tetrahedral Dimers

Structural information is available for a series of edge-bridged tetrahedral dimers of type **1**, having 8, 9, or 10 d electrons per metal, with several examples for each configuration. This provides an ideal opportunity for theoretical investigation of the reasons for structural distortion and the

nature of metal–metal interaction in bridged dimer complexes. We begin with an overview of the structural systematics of this type of molecule.

In describing the structure of a symmetrical tetrahedral dimer, it takes one distance, M–M or M–X, and one interior angle, M–X–M or X–M–X, to fix the geometry of the bridging region. A discussion of direct metal–metal bonding generates a natural emphasis on the M–M separation. But an equally valid focus is on the assembly of the dimer from two monomeric units sharing a tetrahedral edge. The perturbation of metal–metal bonding (or antibonding) then manifests itself as a distortion from the simple edge-sharing geometry. From this point of view the natural emphasis would appear to shift to the deviations of the interior angles from their idealized values shown in **2**. Fully recognizing the interrelation of the angles and dis-


2
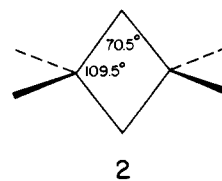
tances, *throughout this paper we will speak of elongation or contraction of the bridging region in terms of the M–X–M angle increasing or decreasing.* A discussion of this angle allows us to put on one scale diverse examples, many different metals and bridging groups, whose similarities and differences perhaps would be difficult to perceive otherwise. In our structures we will also include the MM distance for more complete specification of the bridge region.

Many tetrahedral dimers are known for metals with filled d shells. In metal halide dimers the geometries are quite similar, with examples shown in **3**[6a] and **4**.[6b] Note the elongation

3   **4**
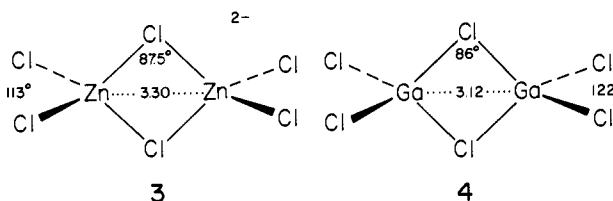
of the bridge region (M–X–M angles greater than 70.5°), and an opening up of the angle between the terminal ligands.[7] The bridge region is presumably stretched by closed shell repulsions.[8] To compensate for the less than tetrahedral angle at the metal one could imagine that sp rehybridization opens up the

angle between the terminal ligands. Yet not all halide bridged d^{10} dimers give the appearance of elongation. Consider for instance the complex **5**, with a relatively short Cu-Cu sepa-

5
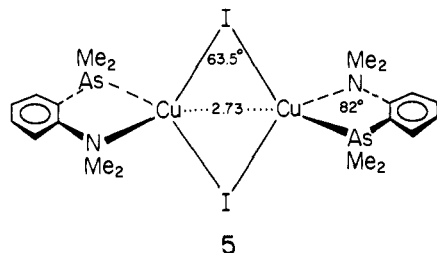
ration and an acute angle at the bridging iodides.[9a] One could again blame rehybridization for the geometrical features—the small external angle imposed by the chelate bite size forcing a larger interior I-Cu-I angle—but perhaps one should first find out what are the geometrical preferences of an unconstrained $I_2Cu(NR_3)(AsR_3)^-$ monomer. The related Zn(II) monomer $(TMED)ZnCl_2$ has a Cl-Zn-Cl angle of 119.4°,[9b] which is not all that different from the I-Cu-I angle of 116.5° in **5**.

Structures of main group dimers can be related readily to the ideal tetrahedron because the ligands are generally of a similar electronic type (there are no strongly π-accepting ligands) and the d levels are usually not involved (they are filled and at lower energy). On the other hand transition metal complexes frequently have both π donor and acceptor ligands, and the high-lying d orbitals are of great importance to both metal–metal and metal–ligand interactions. It is the transition metal complexes that will receive our primary attention.

To begin our series of tetrahedral dimers we have the formally d^{10} species, **6**, the structure of which was determined in

6
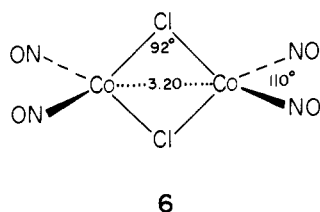
a crystal with some disorder.[10] The metal and chlorine positions are most accurately known, and it is clear that this dimer is also elongated in the bridge region; in fact, more elongated than in the previously mentioned dimetal hexahalides. However, while **3** and **4** are related to tetrahedral MCl_4, the "monomer" of **6**, the hypothetical $Co(NO)_2Cl_2^-$, **7**, will not be an ideal tetra-

7   **8**
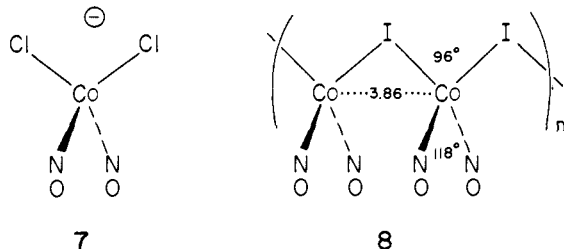
hedron. Distortions prior to dimer formation are likely to be considerable, particularly with the π donor Cl and π acceptor NO on the same metal. In the polymeric dinitrosyl cobalt iodide, **8**, metal–metal repulsions should open the I-Co-I angle.[2j] Yet that angle is 96°, more acute than tetrahedral, and it is the π accepting nitrosyls which spread apart. Such metal–ligand interactions must be considered before the distortions of a dimer can be attributed to metal–metal interactions. This we will do.

There are several complexes structurally similar to **6**, but with two less electrons, among them **9**,[2j] **10**,[12] **11**,[13] and **12**.[14,15] The major difference between the d^9 and d^{10} complexes is the

9   **10**

11   **12**
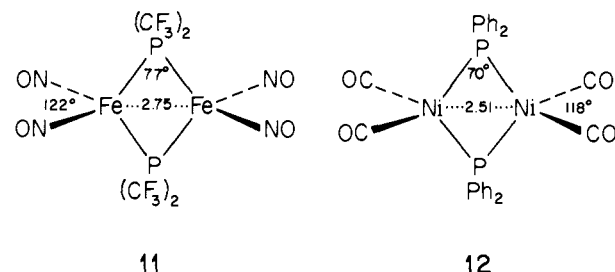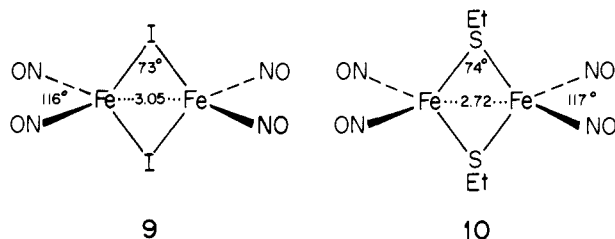
compression in the bridge region. The metal–bridge–metal angles are 70–77°, compared to 92° in **6**. This compression and the 18-electron rule have led to the attractive postulate of a direct metal–metal bond in these molecules. However, note that the compression is accompanied by an increase in the interior angle at the metal. At the same time the external angles between the terminal ligands are greater than in **6**. This is just what one would expect for a d^9 monomer relative to d^{10}. For instance d^{10} ML_4 complexes are regular tetrahedra, while the d^9 $CuCl_4^{2-}$ ion assumes a range of flattened tetrahedral geometries with the precise angle a function of the counterion or crystal packing.[16,17] How much then of the geometry of the d^9 dimers depends on them being built up from d^9 monomer units and how much depends on the direct metal–metal bonding interaction? We will examine this problem. That the monomer geometry is important is signaled by a number of d^9 $X_2MY_2MX_2$ structures which are far from locally tetrahedral at the metal. These include $Cu_2Cl_6^{2-}$,[18] numerous oxo-bridged Cu(II) dimers,[19] the hydride bridged $\{[(C_6H_{11})_3-P(CH_2)_3P(C_6H_{11})_3]NiH\}_2$,[20] and the carbonyl bridged $[(PPh_3)_2 Rh(CO)]_2$.[21] In $Ni_2(CN)_6^{4-}$ there is a very short Ni–Ni bond of 2.30 Å and no bridging.[22a] Similar nonbridged structures are observed for $Pt_2Cl_4(CO)_2^{2-}$ [22b] and $Pd_2(CNCH_3)_6^{2+}$,[22c] both with very short metal–metal bonds.

Among the many dimers with eight d electrons per metal there are three known with locally tetrahedral geometries. These are **13**,[23] **14**,[24] and **15**.[25] In **15** the acetylene is considered

13

14

15
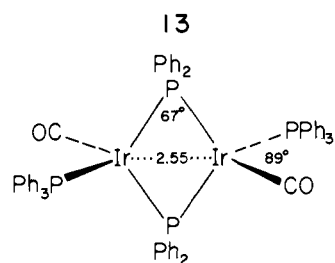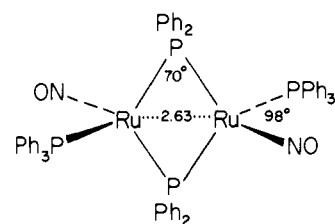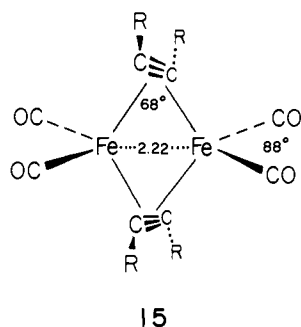
to be one ligand, located at the center of the triple bond.[26] The structures are remarkably similar, given how different the ligands are. Compared to the d^9 dimers, these d^8 binuclear complexes show a further compression in the bridge region and a dramatic decrease of the angle between the terminal ligands. Application of the 18-electron rule leads to the hypothesis of metal–metal double bonds in these dimers, and there is no doubt that direct metal–metal interaction is important.

Yet another interesting aspect of the structure of these molecules is that they are in fact locally tetrahedral rather than square planar at the metal. A low spin d^8 monomer would of course be square planar. Indeed there is a host of molecules and structures of d^8 dimers in which the local coordination at the metal is square planar. These are exemplified by 16[2b] and 17.[27]

16   17
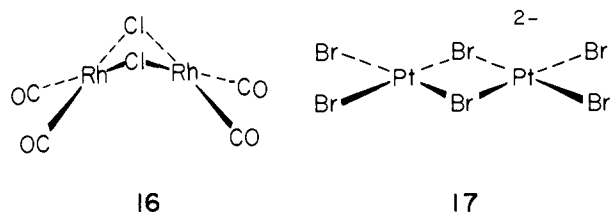
Metal–metal bonding cannot be the sole reason for the assumption of the tetrahedral dimer geometry, since tetrahedral metal–metal bridged structures can be visualized for molecules such as 16 or 17 as well. Still another interesting geometrical preference is expressed in the square planar dimer structures, in that they fall into two groups. Some, like $Rh_2Cl_2(CO)_4$, have the local square coordination planes inclined at an angle to each other,[28] while others, like $Pt_2Br_6^{2-}$, have the two metals and the six atoms directly bonded to them all in one plane.[29]

Finally there are a number of tetrahedral dimers with fewer than eight electrons per metal. Among these are $Co_2Cl_6^{2-}$, d^7,[30] $Ru_2Cl_6^{2-}$, d^6,[31] and Fe_2Cl_6, d^5.[32] The Ru dimer is diamagnetic, and the magnetic properties of the others are, to our knowledge, unknown. Another d^5 system, the sulfide bridged $[C_6H_4(CH_2S)_2FeS]_2^{2-}$, is antiferromagnetically coupled with $J = -148$ cm^{-1}.[33] A related molecule is $[(p\text{-}CH_3C_6H_4S)_2\text{-}FeS]_2^{2-}$.[33] With still fewer electrons one has $[(CH_2SiMe_3)_2\text{-}M(CSiMe_3)]_2$, $M = Nb$, Ta, both diamagnetic.[34a] The structure of the Nb compound has been determined and it has bridging $CSiMe_3$ groups.[34b]

While we have not reviewed all the tetrahedral dimer structures available, perhaps the selection presented is adequate to illustrate the geometrical regularities. The basic problem facing us is to delineate the role of the three factors influencing these structures—monomer geometry, indirect coupling through bridging group orbitals, and direct metal–metal bonding. We begin by a study of the geometrical preferences of a monomer fragment.

Distortions in Tetrahedral Monomers

As a "monomer" model for constructing a dimer $M_2X_2Y_4$ we choose a tetrahedral $X_2MY_2^n$ molecule with whatever charge n is required to make the formal oxidation state of the metal in the monomer equal to that in the dimer. The most
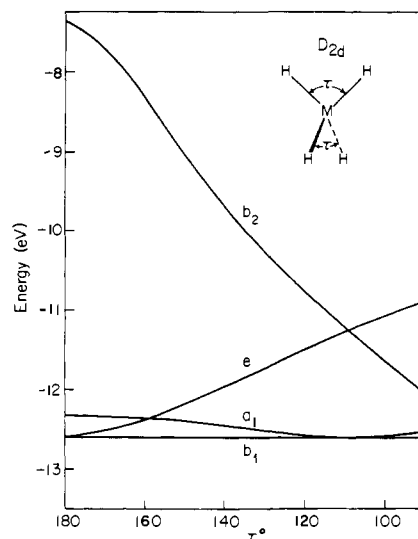

Figure 1. Orbitals of a D_{2d} MH$_4$ MH$_4$ complex as τ is varied.

common substitution pattern among the examples surveyed in the previous section is $X = \pi$ donor and $Y = \pi$ acceptor. We will work up to such a C_{2v} fragment, X_2MY_2, by beginning with the orbitals of a hypothetical MH$_4$ species.

The energy of the d block orbitals of an MH$_4$ complex going from a square planar to a tetrahedral geometry, through a D_{2d} distortion, 18, is illustrated in Figure 1.[17d] The specific ex-

18   19
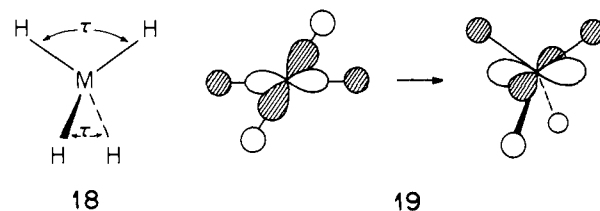
tended Hückel parametrization which we use to generate this figure is described in Appendix 2. Departing from D_{4h}, the high-lying b_2 orbital drops precipitously as overlap with the hydrides decreases, 19. At the same time a pair of e orbitals rises in energy as hydrogens move off the nodes of the xz or yz orbitals[35] and antibonding overlap increases, 20 → 21. This

20   21   22
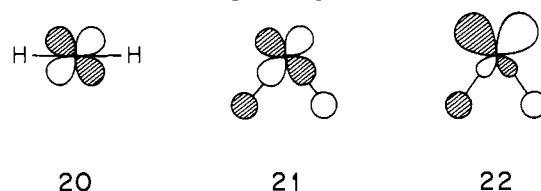
destabilization is relieved somewhat by interaction with a p orbital, which hybridizes the MO away from the hydrogens, 22.[17d] The other orbitals are much less sensitive to this distortion. The xy orbital energy remains constant since the hydrides always lie on the nodes, 23. The z^2 orbital is completely

23   24
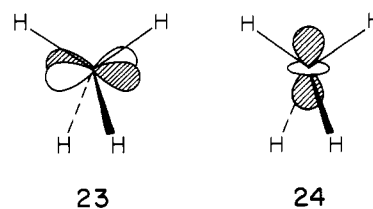
nonbonding in the tetrahedral geometry since the hydrogens also lie on the nodes at this point, 24. As the structure deviates from tetrahedral in either direction, antibonding interaction destabilizes the z^2.

The geometrical implications of this Walsh diagram are
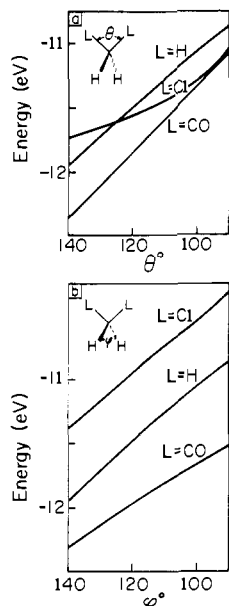
Figure 2. (a, top): Energy of the b_1 orbital in ML_2H_2, L = H, Cl, CO, as the LML angle θ is varied. The HMH angle is fixed at 110°. (b, bottom): Energy of the b_2 orbital in ML_2H_2, L = H, Cl, CO, as the HMH angle φ is varied. The LML angle is fixed at 110°.

Figure 3. Energies of the two a_1 symmetry orbitals of ML_2H_2, L = Cl, CO, and LML angle θ is varied. The HMH angle is fixed at 110°.

clear. A low spin d^8 complex, configuration $(b_1)^2(a_1)^2(e)^4$, will prefer a square planar geometry. A d^{10} complex will be tetrahedral. A d^9 molecule, with one electron in the b_2 orbital, will be poised between the two geometries. It is no surprise that a range of structures is exhibited by d^9 complexes.

This is the story for MH_4. We proceed toward the π bonded X_2MY_2 by studying two sets of limited distortions in H_2ML_2 tetrahedral complexes with L = H, Cl, CO. First, the H–M–H angle was fixed at 110° and the L–M–L angle was varied. In a separate calculation the H–M–H angle was varied while L–M–L was fixed at 110°.

In these C_{2v} complexes the $x^2 - y^2$ and z^2 orbitals are both a_1, the e set from MH_4 splits into b_1 and b_2 (an orbital resembling 22 for each pair of ligands), and the xy orbital has a_2 symmetry.

For d^{10} complexes the major differences in π donors and π acceptors appear in the orbitals of b symmetry. Figure 2a shows the relative changes in the energy of a b_1 orbital of an H_2MI_2 complex as the L–M–L angle is varied, 25. There is an

25   26   27
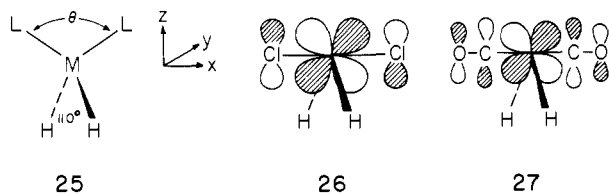
increase in the slope with which the orbital varies with θ along the series L = Cl < H < CO. The orbitals are similar in energy at θ = 90° but separate at wider angles. At an acute angle this b_1 orbital will resemble 22 with only σ effects operating. At wider angles the σ effects diminish and π effects become more important. In H_2MCl_2 the π interaction is repulsive, 26, decreasingly so at smaller θ. This lowers the slope of the orbital in Figure 2a. Another way of describing the effect is to say that as the L–M–L angle diminishes from 180° σ antibonding increases but π antibonding decreases. This is for L = Cl. In contrast the π interaction for L = CO is stabilizing, bonding, as shown in 27. As the C–M–C angle closes, the orbital not only turns on σ antibonding but also loses π bonding. Thus this orbital varies more with θ than the analogous orbital in the chloro complex.
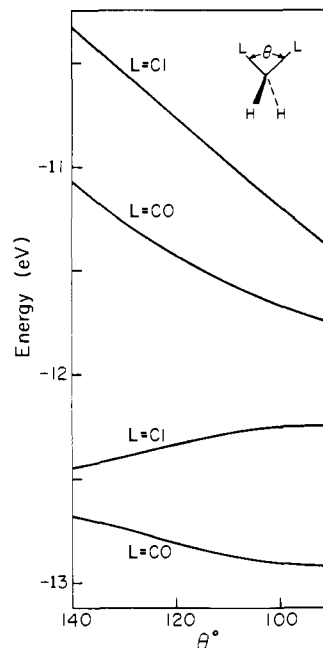
The conclusion that is to be drawn from the different slopes is that for a d^{10} H_2ML_2 at a fixed H–M–H angle the L–M–L angle will be greater between π acceptors than π donors.

Now consider a second distortion, one which varies the H–M–H angle while keeping L–M–L at 110°, 28. The cor-

28   29
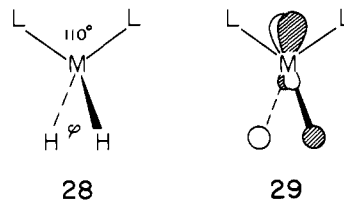
responding changes in the b_2 orbital as a function of φ are shown in Figure 2b. b_2 is the other orbital descended from the MH_4 e set, 29. The slope of this b_2 orbital is smaller for L = CO than for L = Cl. Qualitatively what is happening is that the hybridization of b_2, that is the extent to which a metal p orbital is mixed into yz, increases with decreasing φ. Increased hybridization leads to greater π overlap. Recalling that such π bonding is stabilizing for L = CO, destabilizing for L = Cl, we can understand the behavior of the curves in Figure 2b.

Another way of stating the consequences of the second test motion is to say that in d^{10} H_2ML_2 complexes it is easier to close the angle between two ligands (here hydrogens) when L is a π acceptor than a π donor. Very nicely the two separate motions we analyzed give effects which reinforce each other. We extrapolate with some assurance to the X_2MY_2 complex with X = π donor and Y = π acceptor: In X_2MY_2 complexes the angle between the π acceptors will be greater.

As the b orbitals rise, another orbital, a_1 in C_{2v}, but descended from the b_2 orbital of D_{4h} MH_4, drops. This orbital is mostly $x^2 - y^2$ near the tetrahedral geometry. In d^9 and d^{10} complexes this is the highest occupied molecular orbital (HOMO), and acts as the brake which prevents the complex from opening to a square planar geometry. At lower energy lies another a_1 orbital, largely z^2. Let us consider the effects of the first distortion, defined in 25, for these two a_1 levels. The results are shown in Figure 3. The behavior of the lower a_1 level is easily interpreted. This level is primarily z^2. As such, it is involved in π bonding near the tetrahedral geometry, decreasingly so as the square planar conformation is approached. The
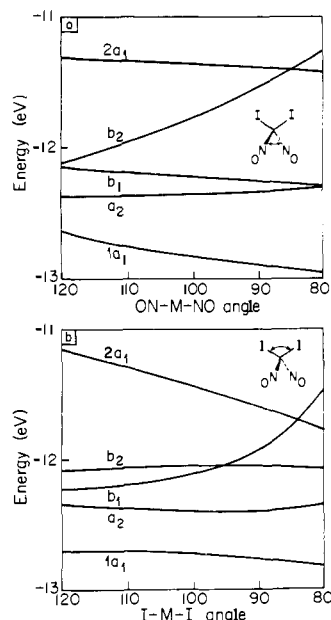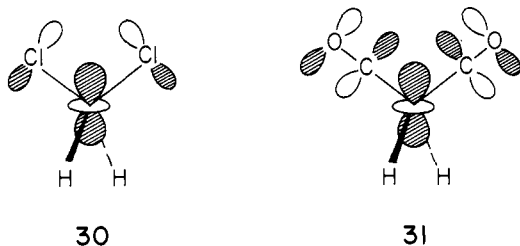
Figure 4. (a, top): Energy levels of Fe(NO)$_2$I$_2$ as the ON–Fe–NO angle is varied. (b, bottom): Energy levels of Fe(NO)$_2$I$_2$ as the IMI angle is varied.

Table I. Calculated M(NO)$_2$I$_2$ and M(NO)$_2$Cl$_2$ Structures

| Compound | Angle | d electron occupation | | |
		10	9	8[d]
M(NO)$_2$I$_2$[a]	I–M–I	97	107	105
	N–M–N	121	124	109
	M–I–M[c]	83	73	75
M(NO)$_2$Cl$_2$[b]	Cl–M–Cl	103	112	105
	N–M–N	120	124	110
	M–Cl–M[c]	77	68	75

[a] Computed with M–N–O = 160°, as in the experimental dimer structure (ref 2j). [b] Computed with M–N–O = 170°, as in the experimental dimer structure (ref 10). [c] Extrapolated dimer bridge angle if two such monomers are superimposed. [d] High spin configuration.

π bonding, shown in **30** and **31**, is stabilizing for L = CO, destabilizing for L = Cl.

30   **31**

The slopes of the higher a$_1$ orbital are influenced by mixing with a still higher-lying a$_1$ orbital, derived from an a$_{2u}$ metal p orbital in square planar MH$_4$. The important role of this orbital has been discussed by us in another context.[17d] The position of this still higher a$_1$ is strongly influenced by the donor or acceptor characteristics of the ligands. For the cases under consideration by us the orbital appears as **32** (L = Cl) or **33** (L = CO). The combination **33** lies at much lower energy than

32   **33**
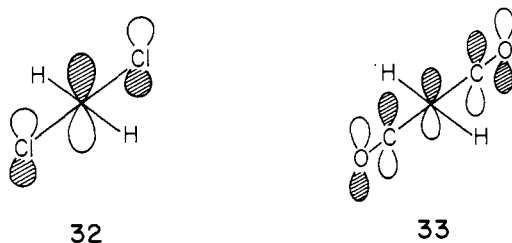
32. Therefore it mixes much more strongly with the a$_1$ whose origin is $x^2 - y^2$, and pushes the latter down as θ increases. This is the reason for the lesser slope of the higher a$_1$ orbital in Figure 3 for L = CO.

The relative π effects on the upper and lower a$_1$ orbitals largely cancel out. For H$_2$MCl$_2$ the upper a$_1$ has a large negative slope and the lower a$_1$ a small positive slope (Figure 3). For H$_2$M(CO)$_2$ both upper and lower orbitals have a small negative slope as C–M–C is closed. For these angular distortions the energy change of both a$_1$ orbitals combined is essentially the same for L = Cl or CO. Filled, this pair or orbitals does not have a differentiating effect on Cl–M–Cl vs. OC–M–CO bending. However, the sensitivity of the H$_2$ML$_2$ upper

a$_1$ to L–M–L bending is much less when L = CO than when L = Cl. Because of this, going from a d^{10} to a d^9 complex (removing an electron from this orbital) will be removing a more severe restraint to the opening of a Cl–M–Cl than a OC–M–CO angle. Thus, whatever the exact geometry of a d^{10} tetrahedral complex, the angle between π donors will open more than between π acceptors if an electron is removed from this orbital.

Having analyzed the separate consequences of π donor or acceptor substitution in H$_2$ML$_2$, we proceeded to test our conclusions on two more realistic complexes with simultaneous donor and acceptor substitution, M(NO)$_2$I$_2$ and M(NO)$_2$-Cl$_2$.[36] Figure 4 shows the d-block levels for M(NO)$_2$I$_2$, calculated for M = Fe. The diagram for M(NO)$_2$Cl$_2$ is very similar. Our conclusions check out for both I–M–I and ON–M–NO angle variation. Thus the b$_2$ orbital affected by ON–M–NO bending has a greater slope than does the b$_1$ orbital involved in I–M–I bending at a similar angle. The a$_1$ ($x^2 - y^2$) is the HOMO for a d^{10} configuration throughout most of the angular range. It is more responsive to I–M–I than ON–M–NO bending.

Next we allowed both X–M–X and ON–M–NO angles to vary simultaneously and computed for various d electron configurations those angles giving the lowest energy. The results are shown in Table I. Note that for all d electron configurations the angle between the π acceptor nitrosyl groups is greater than between the π donor halides. The angles calculated for M(NO)$_2$I$_2$ agree with those found in the Co(NO)$_2$I polymer **8**. Thus we are not surprised by an unusual elongation in dimer **6**, even before considering specifically its electronic structure. The distortions in the monomer tend in that direction.

The point should not be lost that we undertook the analysis of the "monomer" distortions with the eventual aim of probing bonding in the dimer. However, a nice side product of our understanding of these monomer distortions is that we can apply what we have learned to a large group of "real" monomers—tetrahedral d^{10} compounds. For instance, in a number of d^{10} diphosphine dinitrosyl complexes[37] (for instance **34**) as


34   **35**
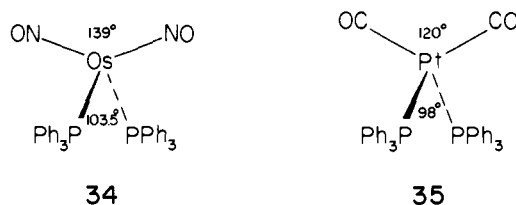
well as dicarbonyls,[38] exemplified by (CO)$_2$Pt(PPh$_3$)$_2$, **35**, as well as mixed carbonyls–nitrosyls,[39] the better π acceptors, NO or CO, are spread apart, in contradiction to what one might have expected on the basis of a steric argument.[40,41]

Copper complexes are known with two phosphine and two π donor ligands in which it is the phosphines which spread apart.[42] However, all of these involve chelates or bridge systems in which the donor–metal–donor angle is restricted, so that sp hybridization effects could be responsible.[43]

Still another distortion that occurs in the dinitrosyls is some departure of the M–N–O unit from linearity. We think that we understand the origins of this deformation. The nitrosyls should bend toward each other at a small N–M–N angle, away from each other at a large N–M–N angle. The argument is given in Appendix 1.

If one electron is removed from our X_2MY_2 models, it will come from the high lying a_1 (mostly $x^2 - y^2$) orbital. This orbital rises sharply as the angle between donors is increased, but is less sensitive to the angle between acceptors. Thus in a d^9 relative to a d^{10} complex the angle between π donors should increase, but that between π acceptors less so.[44] Our calculations on $M(NO)_2X_2$ complexes indicate that for $X = Cl$ or I the X–M–X angle will open by 9–10° in going from a d^{10} to a d^9 metal. The angle between the nitrosyls, however, will open only 4° for $X = Cl$ and 3° for $X = I$. Note for further reference that these are also the changes observed in going from the cobalt dimer, 6, to the iron dimers 9–11.

Were a second electron removed from the upper a_1 orbital to give a d^8 diamagnetic complex, the result would be a square planar structure. An alternative is a high spin d^8 species in which the second electron is removed from the highest orbital of b symmetry, the orbital pushed up by the antibonding interaction, 36, with the strongest π donor. As noted above, this
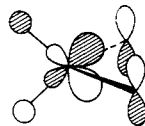
36

orbital is highly sensitive to the angle between the other ligand pair. Removing one of the b electrons on going from d^9 to high spin d^8 releases a severe restraint on that angle. The weakest π donors or the strongest π acceptors should draw closer together in a high spin d^8 (relative to d^9) complex, while the angle between the best π donors should be relatively unchanged.

The calculated geometries of high spin d^8 $M(NO)_2X_2$ (Table I) behave as expected, the ON–M–NO angle decreasing sharply while the X–M–X angle remains almost unchanged. Experimentally, in the high spin Ni(II) complex $(Ph_3P)_2NiBr_2$ the angle between the π donor bromines is 123° while that between the phosphines is an acute 110°.[45a] Some related cases are also consistent.[45b-d]

The previous analysis has been directed toward the effect of π-donors and acceptors on the angular distortions in a tetrahedral complex. The σ effects have been by-passed simply because the known dimers are substituted with π active groups such as Cl, NO, CO. We now return to the role of σ-donation and acceptance.

Let us go back to MH_4 and open up one angle θ, defined in the same way as it was in 25. The metal orbitals strongest affected by this motion are the metal xz and $x^2 - y^2$. z^2 is mildly moved and xy and yz by symmetry remain at constant energy. The effect of σ donation or acceptance may be simulated by varying the energy of the two ligand orbitals being moved. In the calculations this is easily done by changing the H_{ii} of the two hydrogens. Both $x^2 - y^2$ and xz are lowered in energy as the ligands moved are made worse σ donors (lower H_{ii}, more electronegative) and both are raised when the ligands are made better σ donors (higher H_{ii}, more electropositive) than the remaining two hydrogens. But the differential effect is greater on the xz orbital. Its slope is diminished for a worse σ donor,
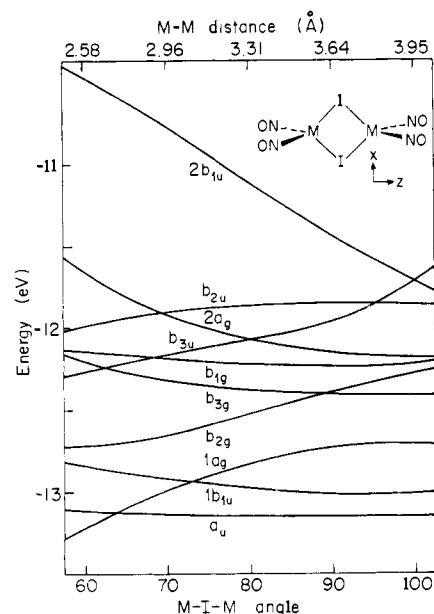

Figure 5. The ten d block levels of $M_2(NO)_4I_2$ as a function of M-I-M angle θ. A nonlinear M-M distance scale is indicated at the top.

increased for a better σ donor. Through this controlling effect we come to the conclusion that *in a d^{10} tetrahedral complex the angle between the better σ donors will be increased, that between the worse σ donors decreased from the reference tetrahedral angle.*

At times the π and σ effects may conflict. For instance in diphosphine dinitrosyl complex 34 the phosphine is clearly the better σ donor and nitrosyl the better π acceptor. In this case the π effect clearly dominates and the N–M–N angle is wider than the P–M–P angle.

With less π active groups it is difficult to assess the relative merits of σ donation and π acceptance. Perhaps the σ effect is relevant to the geometry of the iodide bridged Cu(I) dimer, 5. If we choose as a drastically simplified monomer model $I_2Cu(NH_3)_2^-$ and optimize its geometry, we obtain N–Cu–N 96°, I–Cu–I 126°. We think this distortion is dominated by the relative electronegativity or σ donation effects, but obviously the steric bulk of the I ligands could be playing a role. If the dimer $(NH_3)_2CuI_2Cu(NH_3)_2$ is constructed as a simple superposition of the calculated monomer units, it would have a Cu–I–Cu angle of 54°. So the observed angle of 63.5° in 5 may actually represent an elongation!

There is no question that the molecular orbital argument leading up to our general conclusion for Y_2MX_2 geometries is a labored one. We were persistent in seeking the argument out, for in dealing with approximate molecular orbital calculations of the extended Hückel type one definitely needs the supporting structure of a symmetry and overlap based explanation. We proceed to combine the X_2MY_2 units to form the dimers.

The Electronic Structure of the Dimers

The behavior of all the d levels of $M_2(NO)_4I_2$ on deformation of the bridge is shown in Figure 5. D_{2h} symmetry is maintained throughout. The rise and fall of all those levels gives a messy appearance to this figure, but hidden in it is a great deal of order. First we draw a schematic representation of the d orbitals at some realistic bridging geometry. This is done in Figure 6. The levels are not arranged in order of energy here, but are grouped in pairs according to their metal character. One immediately recognizes that these ten orbitals are symmetric (S) and antisymmetric (A) combinations, with respect to the xy plane, of the monomer orbitals we have just consid-
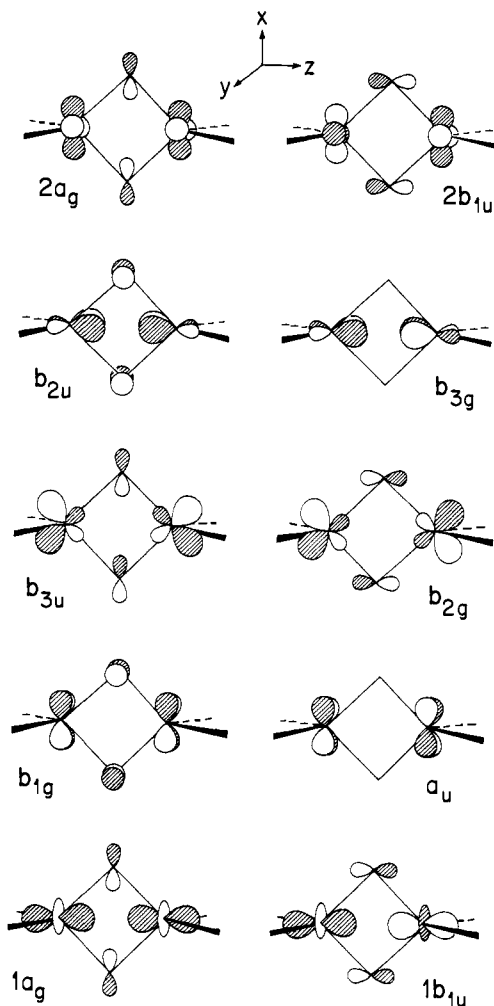
Figure 6. Schematic drawing of the ten d block orbitals of $M_2(NO)_4I_2$. Mixing of z^2 and $x^2 - y^2$ occurs in all a_g and b_{1u} orbitals. especially in $2b_{1u}$. The levels are shown in matched pairs.

Figure 7. Average energies of the symmetric-antisymmetric pair of orbitals in $M_2(NO)_4I_2$ as a function of I–M–I angle. The level energies which come from Figure 5 and are summed for the horizontal pairs in Figure 6. A nonlinear M–M distance scale is indicated at the top, and an M-I-M scale at bottom. This drawing is to be compared to Figure 4b.

ered: b_{1g} and a_u are derived from the xy orbital a_2, $1a_g$ and $1b_{1u}$ primarily from the z^2 a_1, $2a_g$ and $2b_{1u}$ mainly from the $x^2 - y^2$ a_1, b_{2u} and b_{3g} from the yz b_2, b_{3u} and b_{2g} from the xz b_1. Each combination mixes into itself in an antibonding manner appropriate symmetry orbitals of the bridging halogens.

Since the dimer levels so obviously come in S and A pairs of monomer levels, it suggests itself that it would be informative to replot Figure 5, pairwise summing the energies of the symmetry related S and A orbitals. The result is shown in Figure 7. We ask the reader to compare Figure 7 with the earlier Figure 4b, in which the orbitals of the $M(NO)_2I_2$ monomer were plotted as a function of the I–M–I angle. The resemblance is remarkable. It is difficult to escape the conclusion that the response of the average energy of each S–A pair in the dimer to an angular distortion is essentially the same as the response of the monomer model.

The individual level slopes in the dimer are important in their own right, especially the higher levels which will set the geometry of the d^8 and d^9 dimers. In general the energy ordering and slopes of each level pair are set by the usual factors of direct (through-space, metal-metal bonding) and indirect (through-bond coupling, superexchange) interaction. Let us examine them one by one. The xy pair a_u and b_{1g} maintains a fairly constant splitting as a function of M–I–M angle, with a_u always below b_{1g}. This is consistent with a dominant through-bond coupling, for a_u finds no symmetry match among bridging halogen orbitals, but b_{1g} is destabilized by interaction with a halogen p_y combination. The through-space or direct
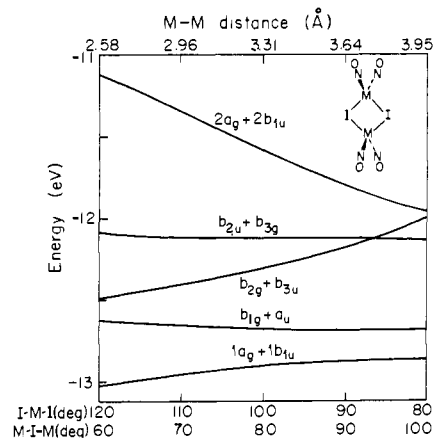
metal–metal interaction is δ type and not significant at realistic metal–metal separations.

The b_{2u}–b_{3g} pair starts out at a large M–I–M angle (long M–M) with b_{2u} (S) above b_{3g} (A). This is again through-bond coupling at work, with halogen orbitals destabilizing the b_{2u} combination. But b_{2u} is metal–metal π bonding and b_{3g} is metal–metal π antibonding. As the M–I–M angle drops and correspondingly the metal atoms come together, the direct overlap stabilizes b_{2u} and destabilizes b_{3g}. The two levels cross at M–I–M < 60°. The through bond coupling pattern also sets the order b_{2g} (A) below b_{3u} (S) in the xz pair. Because of the hybridization apparent in Figure 6, the through-space interaction is turned on only slowly, and the crossing of these π bonding levels occurs to the left of Figure 5.

Direct and indirect effects are also operative in the levels descended from the monomer a_1 pair—a_g and b_{1u} in the dimer D_{2h} symmetry. Their analysis is somewhat complicated by the presence of two a_g and two b_{1u} levels. The mixing of the two could be seen in the comparison of Figures 7 and 4a, where the lower $1a_g + 1b_{1u}$ energy sum fell more steeply than the lower a_1 in Figure 7, while the upper $2a_g + 2b_{1u}$ sum rose more sharply with decreasing M–I–M angle. A consequence of this mixing is that in each level z^2 and $x^2 - y^2$ mix, and this will subsequently have an impact on our discussion of the evidence for direct metal–metal bonding in the d^9 dimers.

We proceed to examine the bonding in d^{10}, d^9, and d^8 dimers using the information of Figure 5. In the d^{10} dimers all ten levels are occupied. The result is a slight repulsion that elongates the dimer relative to the single metal complex. The calculated M–X–M angles of the d^{10} $M_2(NO)_4X_2$ complexes are 94° for X = I and 92° for X = Cl, compared to 83° and 77° estimated from superimposing the calculated monomer geometries, Table I. We have already pointed out that the geometry of **6** is unusually elongated,[10] with a Co–Cl–Co angle of 92°, because the metal–ligand interactions in the monomer tend in that direction.

If each metal center carries nine d electrons, then the highest energy orbital in Figure 5, $2b_{1u}$, will be vacant. The gap between this orbital and the next highest level is nearly 1 eV at M–I–M = 75°, which should be sufficient to ensure a low-spin diamagnetic complex, as is observed in the cited examples **9–12**.

The $2b_{1u}$ orbital rises sharply as the bridge angle is closed. Thus, when this orbital is vacant, the angle should be smaller than when it is filled. Our calculated geometries do show this trend. The optimum M–X–M angles calculated for d^9 com-

plexes are 76° for X = I and 74° for Cl compared to 94° and 92° in the d^{10} complexes. Experimentally the 73° angle in $Fe_2(NO)_4I_2$, **9**,[2j] is also more acute than the 92° angle in $Co_2(NO)_4Cl_2$, **6**.[10]

Is there a direct metal–metal bond in these d^9 complexes? Yes and no. Since the b_{1u} orbital rises steeply as the bridge region is compressed and the metals approach one another, there is a temptation to say that this LUMO of the d^9 dimer is primarily a metal–metal antibonding orbital. If that is so, it should have a bonding counterpart which decreases in energy with decreasing metal–metal separation. $2a_g$ would be one candidate for this bonding role, but, as one can see in Figure 5, it does not have the desired slope. Moreover, $2a_g$ is more δ-like than σ over a large range of angles. This was implied in the schematic drawings of Figure 6 and is made more specific by Table II, which lists the composition of the a_g and b_{1u} levels of the dimer as a function of M–X–M angle.

If $2a_g$ is not a good candidate for the metal–metal σ bond, we must consider the lower $1a_g$. This orbital is primarily z^2 and so better fits the σ specification. It falls in energy with decreasing metal–metal distance. If any level is to be identified as the metal–metal σ bond, this must be the one.

Nevertheless, we remain hesitant about saying that direct metal–metal interaction is responsible for the compression of the bridging region in the d^9 complexes. First, when we examine the energy of not only the $1a_g$ but the entire block of occupied a_1 orbitals, $1a_g + 1b_{1u} + 2a_g$, we find that the contribution of the six electrons is almost independent of the bridge angle. Second, and more important, the calculated and experimental $M(NO)_4X_2$ dimer structures, as measured by the interior angles, are close to the structures expected from edge sharing $M(NO)_2X_2$ monomers. For instance in $Fe_2(NO)_4I_2$ we calculate an optimum Fe–I–Fe angle of 76°. The experimental angle is 73°. Edge sharing of undistorted monomer fragments (Table I) would lead to an extrapolated Fe–I–Fe angle of 73°. All these values are close to each other, and we do not see much evidence of a special extra contraction due to metal–metal bonding.

We must now consider the diamagnetic dimers with eight d electrons per metal, **13–15**. Reasoning back from the fact that the angle between the terminal ligands in these dimers (88–100°) is much smaller than in the d^9 complexes (116–122°), we infer that the second vacant orbital must rise as those angles close. The b_{2u} and b_{3g} orbitals (Figure 5, redrawn in **37**

37, b_{2u}   **38, b_{3g}**
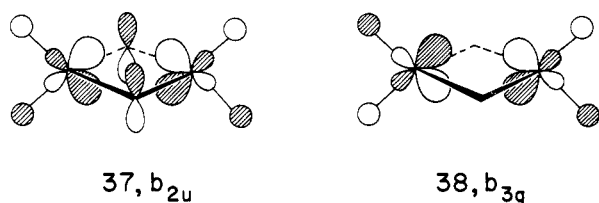
and **38**) fulfill this requirement. In Figure 5 these levels are buried among the other d orbitals. However, as the terminal ligands move closer together, the average energy of the b_{2u} and b_{3g} will rise much as the b_2 orbital does in the monomer (Figure 4a).

The d^8 tetrahedral dimers which are known have either phosphido or acetylene bridges, **13–15**. We therefore went over to a different model compound, $Rh_2(CO)_4(PH_2)_2$. Figure 8 shows the way that the energy levels for this model vary with deformation of the bridge region. The b_{3g} and b_{2u} orbitals lie below the highest $2b_{1u}$ level. The levels are nicely separated (1.4 eV at M–PH_2–M = 70°) with the metal–metal π-bonding b_{2u} orbital at lower energy. The diamagnetism of the d^8 dimer with $2b_{1u}$ and b_{3g} orbitals vacant is assured. The phosphido bridged dimers have also been the subject of an excellent study by Burdett,[46] where similar level orderings are obtained.
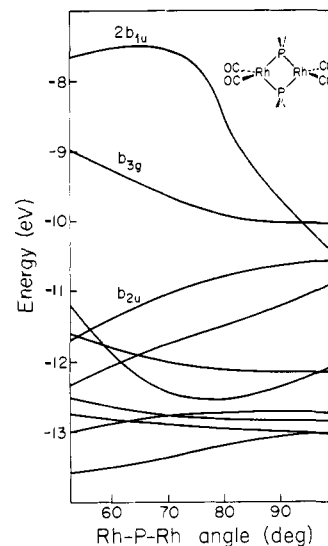

Figure 8. Energy levels of tetrahedral $Rh_2(CO)_4(PH_2)_2$ as a function of Rh–P–Rh angle. Only selected levels are identified by symmetry type.

Table II. Occupation of Specified Metal Atomic Orbitals in $Fe(NO)_4I_2$

MO	AO[a]	% of electron density on both metals at specified M–I–M angle			
		60°	70°	80°	90°
$2b_{1u}$	$s + z$	2	6	9	11
	$x^2 - y^2$	28	23	26	32
	z^2	26	30	26	21
$2a_g$	$s + z$	16	13	11	9
	$x^2 - y^2$	32	45	58	68
	z^2	9	8	8	9
$1b_{1u}$	$s + z$	10	3	3	2
	$x^2 + y^2$	9	7	4	1
	z^2	38	45	53	60
$1a_g$	$s + z$	0	2	3	5
	$x^2 - y^2$	5	5	4	0
	z^2	62	53	44	38

[a] We have added together the population of the metal 4s and 4p orbitals.

That the b_{2u} and b_{3g} levels are so nicely split apart in energy is not a consequence of the smaller OC–Rh–CO angle. That angle assures the rise in energy of the b_{2u}–b_{3g} pair, but not their relative ordering, which in our $Fe_2(NO)_4I_2$ calculations was b_{3g} below b_{2u}, with a level crossing at M–I–M < 60°. The slopes of the b_{2u} and b_{3g} levels are similar in $Fe_2(NO)_4I_2$ and $Rh_2(CO)_4(PH_2)_2$, but their ordering differs. The change in ordering must come about as a result of the change of the bridging ligands from I or Cl to PH_2. This was probed by a calculation on a hypothetical $Rh_2(CO)_4Cl_2$ (the real molecule has a very different structure, **16**) in which the OC–Rh–CO angle was the same as in $Rh_2(CO)_4(PH_2)_2$. The results are shown in Figure 9. Both b_{2u} and b_{3g} are at higher energy, but their ordering is similar to that in $Fe(NO)_4I_2$. The hypothetical tetrahedral $Rh_2(CO)_4Cl_2$ would be a triplet ground state.

Here we see clearly the consequences of a differential through bond coupling effect. The orbitals of the Cl and PH_2 bridges obviously have a major effect on the energy ordering of the higher levels of the dimer. It is important to analyze what has happened.

Referring back to **38**, we note that as a first approximation the b_{3g} orbital is not affected by the bridging ligands. Indeed a comparison of Figures 8 and 9 shows that the b_{3g} level is essentially identical in the two cases. The b_{2u} level does mix into
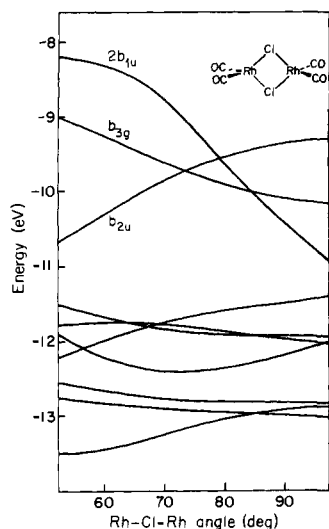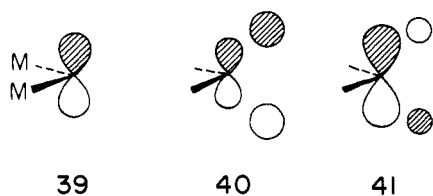
Figure 9. Energy levels of tetrahedral $Rh_2(CO)_4Cl_2$ as a function of Rh–Cl–Rh angle. Only selected levels are identified by symmetry type.

itself ligand orbitals—in the halogen bridge case a lone pair **39**, in the PH_2 bridge case the PH σ and σ^* orbitals **40** and **41**.


In the Cl bridged dimer the lone pair **39** mixes with the metal d orbitals in an antibonding manner, destabilizing the b_{2u} orbital. In the PH_2 bridged dimer the σ bonding orbital **40** plays a similar role, but interacts less strongly because it is localized more on the PH_2 hydrogens. The σ^* orbital **41** is relatively low lying and concentrated on the phosphorus. It mixes with the metal d orbitals in a stabilizing manner. In our calculations the opposing interactions with **40** and **41** nearly cancel, and b_{2u} always lies below b_{3g}, even at large metal-metal separations.

The b_{2u} and b_{3g} orbitals are primarily composed of hybrids on one metal pointing toward the other one. There is significant metal-metal overlap, even at large metal-metal separations. This accounts for the significant slopes of the b_{2u} and b_{3g} levels in Figure 8 or 9. *A metal-metal π bond exists in the equilibrium geometry of these dimers.* Concerning the σ bond in the same molecules, we are left with the same ambiguity that bedeviled our consideration of $Fe_2(NO)_4X_2$.

Square Planar vs. Tetrahedral Dimers

The question was raised earlier as to why some d^8 dimers are "tetrahedral", like **13**, whereas others are "square planar", like **16**. We now examine the question in the context of alternative geometries **42a** and **42b** for $Rh_2(CO)_4X_2$, X = Cl, PH_2. We
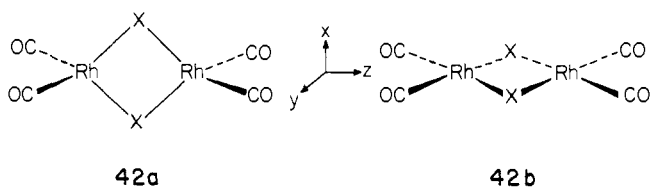

noted earlier that the locally square planar d^8 complexes come in two types, all planar, as shown in **42b**, and with the coordi-

nation planes inclined relative to each other, as in the actual structure of $Rh_2(CO)_4Cl_2$, **16**. The next section will discuss this "hinge" type of distortion, but for reasons of simplicity in comparing the tetrahedral and square planar extremes we assume in this section the D_{2h} structure **42b**.[47]

The simplest intramolecular motion which interconverts the two D_{2h} forms **42a** and **42b** is a concerted twisting of the two bridging ligands (or the four terminal groups) around the metal-metal axis. This motion was considered in our earlier discussion of $Cu_2Cl_6^{2-}$.[1b] The intermediate symmetry is C_{2h}. We have constructed potential energy surfaces for these twists. Their presentation is complicated by the fact that the optimum angles at the bridge are very different in the two extremes. For instance, for X = Cl Rh–Cl–Rh = 50° in the tetrahedral geometry, but 97° in square planar. For X = PH_2 Rh–P–Rh is calculated as 64° in tetrahedral, 102° square planar. Instead of presenting a curve that shows an actual twisting energy, we show a correlation diagram, Figure 10, for $Rh_2(CO)_4Cl_2$ between the above cited optimum geometries in either extreme. The compression-elongation does not break the C_{2h} symmetry.

The most striking feature of this diagram, as well as of the one for $Rh_2(CO)_4(PH_2)_2$ is that the twisting motion is accompanied by a level crossing. It is a symmetry forbidden reaction. The vacant levels on the tetrahedral side are b_{1u} and b_{3g}. On the square planar side they are obviously the symmetric and antisymmetric combinations of metal xz, **43a** and **43b**, b_{2u}
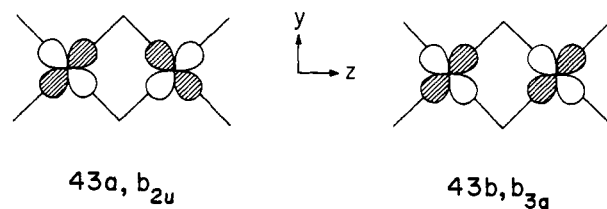
and b_{3g}. One of these levels correlates across, but the other one does not. The immediate implication is that the existence of isomeric d^8 dimers, square-planar and tetrahedral, separated by a sizeable activation energy, is in principle a possibility. This interesting prediction is tempered by our realization that the interconversion of the extreme forms **42a** and **42b** need not necessarily proceed by a simple twist. Alternatively it could come about by an associative equilibrium with other ligands, or by rupture of a single M–X bond.

We still have not answered the question as to why the chloro bridged dimer prefers to be square-planar while the phosphido bridged molecule is tetrahedral. Although metal-metal bonding favors tetrahedral dimers, it is not the sole reason for the different geometries of halide and phosphido bridged complexes. Even if the b_{2u} (π) orbital is occupied in a tetrahedral $Rh_2(CO)_4Cl_2$ complex, the square planar dimer is still lower in energy by 2.3 eV at the respective minima. The phosphido bridged complex, on the other hand, prefers the tetrahedral structure by 0.55 eV over the square planar one. If one compares the PR_2 and Cl ligands, one comes to the conclusion that they differ most in those orbitals which are out of the MXMX plane. We focus our attention on these.

There are two metal orbitals which can interact with out-of-plane bridge ligand wave functions. These are the b_{2u} and b_{1g} combinations of Figure 6 (b_{2u} is also shown in **37**). The corresponding orbitals in the square planar complex are **44** and **45**. In **44**, the square planar counterpart of **37**, the d orbitals
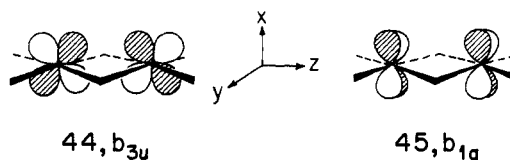
are no longer in the plane of the terminal ligands. As a result, they are not hybridized toward the center of the bridge system, and so will interact less with the bridge ligand orbitals. At Rh–X–Rh = 101.2°, **44** with Cl bridges is 0.51 eV above the equivalent with PH_2 bridges. In the tetrahedral geometry (Rh–X–Rh = 67.8°) **37**, with X = Cl, is 1.16 eV above the orbital with X = PH_2. With two electrons in these orbitals the difference amounts to a 1.3 eV greater preference for the square planar dimer when X = Cl instead of PH_2.

The tetrahedral b_{1g} and **45** do not differ in hybridization, but do have considerably different M–X–M angles. This is illustrated in a somewhat exaggerated manner in **46** and **47**.

46   **47**

The bridge–metal π bonding is greater in the tetrahedral geometry. In the square planar dimer the energy of **47** is 0.66 eV higher with Cl bridges than with PH_2 bridges. In the tetrahedral dimer with Cl bridges, **46**, is 1.11 eV above the orbital with PH_2 bridges. With two electrons in these orbitals the interactions with Cl bridges again favor the square planar geometry more than the same interactions with PH_2. This time the difference is 0.9 eV.

The tendency for the dimer to adopt a square planar rather than tetrahedral structure is 2.88 eV greater in $Rh_2(CO)_4Cl_2$ than in $Rh_2(CO)_4(PH_2)_2$. Of this difference most (~2.2 eV) arises from the out-of-plane interactions we have just described.

The similarity of the acetylene bridged complex **15** to the other dimers is now obvious. Acetylene has no high-lying filled orbitals which are antibonding between the carbons. Such "out-of-plane" orbitals could push the geometry toward square planar, just as they do in the $Rh_2(CO)_4Cl_2$ case. In general we would expect any d^8 four-coordinate dimer to be tetrahedral about the metals if the bridging ligands are *not* π donors. In particular $Rh_2(CO)_4(PR_2)_2$ should be tetrahedral, in contrast to $Rh_2(CO)_4Cl_2$. If the bridging ligands are good π acceptors, then other distortions, to be discussed below, may yet occur.

The Hinging Distortion in Square Planar Dimers

In the geometries of locally square planar d^8 dimers one notices a variation in the "hinge" angle λ, the dihedral angle between the local coordination planes. In many molecules λ = 180°,[29] but in a significant subset λ is less than 180°, or the

48   **49**

molecule is hinged.[28,48] The structures themselves hint that the energies involved in this particular deformation are small, for electronically quite similar species are sometimes planar, sometimes hinged. For instance, in the ubiquitous Pd(II) halide bridged allyl complex series, **49**, one has planar geometries for the following allyl substitution patterns: 2-methyl,[29i] 1,1,3,3-tetramethyl,[29i] 2-neopentyl,[29h] cyclobutenyl,[29g] and the unsubstituted allyl;[29f] while 1,2,3-trimethyl,[28l] 2-methyl-1-*tert*-butyl,[28l] 1,3-dimethyl,[28k] and cycloheptenyl[28m] are all hinged. Among the Rh(I) chloride bridged dimers
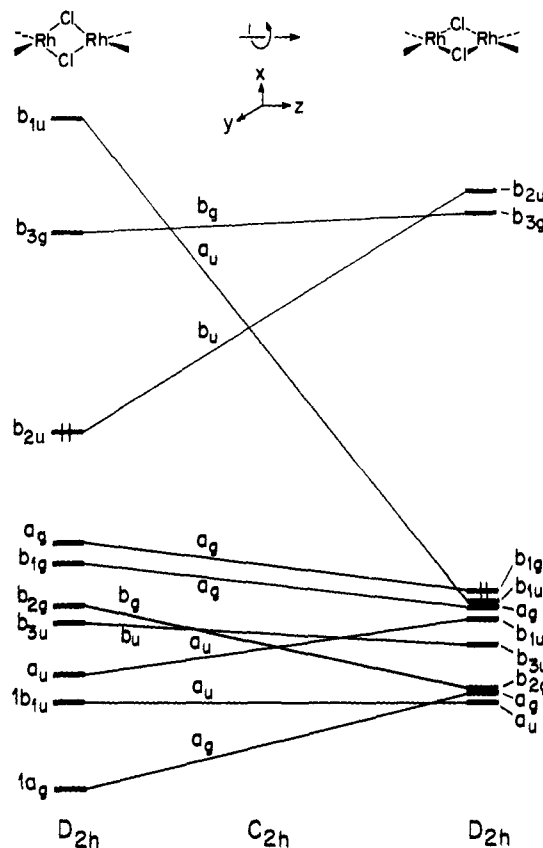

Figure 10. A correlation diagram between tetrahedral (left) and square planar (right) $Rh_2(CO)_4Cl_2$. The HOMO is b_{2u} at left and b_{1g} at right.

$X_2RhCl_2RhY_2$ one has a planar structure for X_2,Y_2 = cyclooctal-1,5-diene[29b] but a hinged one for X_2 = cyclooctal-1,5-diene, Y = $P(OPh)_3$,[28g] X,Y = ethylene,[28f] X,Y = CO,[2b] X_2Y_2 = 4-methylpenta-1,3-diene,[28h] and X = CO, Y = PMe_2Ph.[28i]

We have studied the hinging distortion for a model $Rh_2Cl_2(CO)_4$, which has been examined by Burdett as well.[46] The calculated equilibrium geometry in our calculations is planar, λ = 180°. This is not the correct geometry, which in the solid state has λ = 124°. However, the computed variation of the energy with λ gives the expected picture of a soft motion. To deform from λ = 180° to λ = 140° costs 3.1 kcal/mol, to λ = 120° 7.5 kcal/mol. The way that the individual energy levels vary with λ is shown in Figure 11. There is no obvious controlling orbital in the picture. Some levels move up, mainly those antisymmetric with respect to the *yz* plane; some move down, mainly the symmetric ones. But the overall effect is slight. The bridging chlorines provide effective coupling between the metal orbitals over a wide range of λ. The softness of the potential energy curve for hinging was checked by varying the bridging ligand X in $Rh_2X_2(CO)_4$. For instance for X = PH_2 a bent molecule, λ ~120°, was preferred to a planar one by approximately 9 kcal/mol. Unfortunately we see no way at this time to predict whether a given d^8 dimer will be hinged or planar. Steric and crystal packing forces are likely to be determinative, for there is no large identifiable electronic effect influencing this distortion.

Dimers with Fewer Electrons and Unusual Geometries

The previous sections have dealt with tetrahedral d^8, d^9, and d^{10} dimers and square planar d^8 species. We turn briefly to a discussion of the tetrahedral dimers with fewer than eight d electrons and conclude with an account of some less typical geometries.
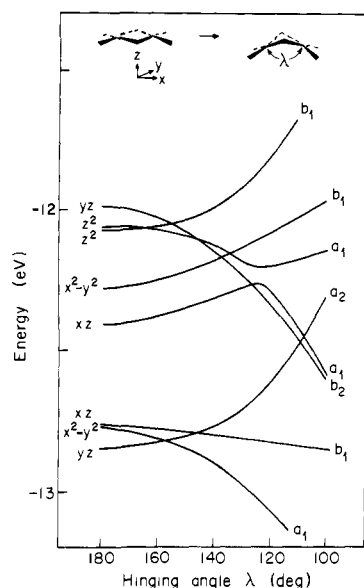
Figure 11. Variation in energy of the d block levels with the hinging angle λ in $Rh_2(CO)_4Cl_2$. The primary d orbital contributing is indicated at left. Note that the coordinate system is appropriate to the C_{2v} symmetry maintained, but differs from that used above for the square planar dimers.

$Co_2Cl_6{}^{2-}$ has been observed as a counterion in a cyclohexaphosphazene structure,[30] and Fe_2Cl_6 as a gaseous species.[32] Their structures are shown below. Our calculations indicate that for both molecules the d band is little differentiated—in **50** the ten d orbitals spread out over a range of 1.7
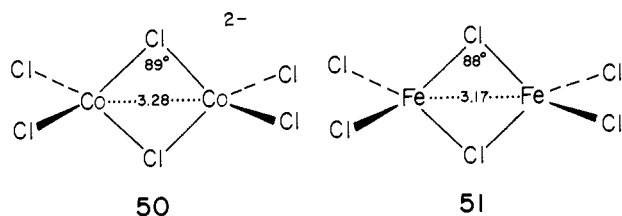
eV, in **51** over 2.0 eV. The ordering of the levels differs significantly from that shown in Figure 5, in that the π type b_{3u} and b_{2u} levels join $2a_g$ and $2b_{1u}$ near the top of the band. This is a consequence of π-antibonding with terminal chlorines. Whatever the level ordering, the spacing of the levels is close. We are not able to predict quantitatively the extent of the magnetic coupling to be expected in these molecules, but we would not anticipate a large J in either the d^5 or the d^7 dimer. We have not studied $Ru_2Cl_6{}^{2-}$, which is diamagnetic, with a Ru–Cl–Ru angle of 87.4° and a Ru–Ru distance of 3.26 Å.[31]

Holm and co-workers have synthesized several sulfide bridged tetrahedral dimers of Fe(III) in their elegant studies of analogues for the active sites of nonheme iron–sulfur proteins. These are of the general type **52**, with the geometry indicated for $R = p$-tolyl.[33] Our calculations modeled this structure with $R = H$. The d band was split over some 2.9 eV, with a significant 1 eV gap between the three highest levels and the lower seven. The three high-lying levels are $2b_{1u}$, b_{3u}, and

b_{2u}. The lower seven levels are close together, and their spacing is to some extent sensitive to the Fe–SR torsion angle. Again we cannot predict the magnitude of the magnetic coupling, except to say that a very large negative J is unlikely and that the maximum magnetism should correspond to four unpaired spins. The experimental facts are more definitive in giving a $J = -148$ cm^{-1}.[33]

An unusual carbyne bridged series of complexes of Nb and Ta has been synthesized by Mowat and Wilkinson.[34a] A structure of one compound was determined[34b] and is shown in **53** ($R = SiMe_3$). If the CR bridge is viewed as triply nega-

53
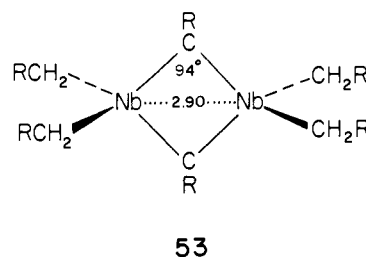
tive, this is formally a Nb(V) d^0 complex. We studied a model compound with $R = H$. Though the charge on Nb is far from +5, this is like a d^0 complex in that ten orbitals, identifiable as primarily d, are vacant. Our calculations fully support Wilkinson's view that this is a quasi-aromatic system. The carbyne lone pairs donate to the appropriate symmetry Nb d orbitals, as shown in **54a** and **54b**. A gap of 1.3 eV between the

54a   **54b**
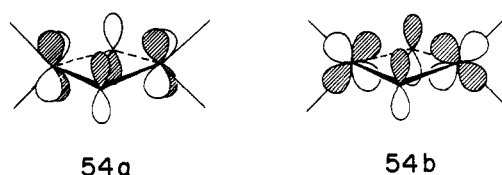
HOMO and the bottom of the d band is sufficient to yield a diamagnetic complex.

There is a set of d^9 dimers that do not bridge but form direct metal–metal bonds. $Ni_2(CN)_6{}^{4-}$ and $Pd_2(CNCH_3)_6{}^{2+}$ have had their structures determined.[22a,c] Each metal is nearly square planar, and the coordination planes are twisted by approximately 90° relative to each other, as shown schematically in **55**. The Ni–Ni separation is very short, some 0.2 Å shorter

55
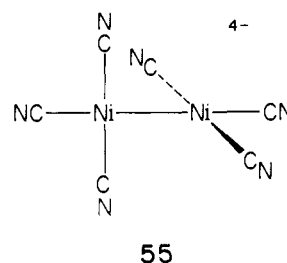
than the supposedly Ni–Ni single bonded bridged dimer **12**. The Pd dimer also has a short Pd–Pd distance of 2.53 Å. $Pt_2(CO)_2Cl_4{}^{2-}$ has a related structure, but with the coordination planes forming an angle of 60° and the carbonyls transoid.[22b] It also has a short Pt–Pt separation of 2.58 Å.

Our calculation on $Ni_2(CN)_6{}^{4-}$ in an idealized geometry close to that observed in the crystal structure[22a] yielded a picture typical of square planar d^8 systems. A sizeable gap of 2.6 eV separated filled from unfilled levels. A potential energy curve for torsion around the Ni–Ni bond is shown in Figure 12. There is little resistance to a small twist from the observed orthogonal form, but a large barrier to making the molecule planar. The source of that barrier is traced by us to the expected steric repulsion. When those repulsions are removed by incorporating the ligands in a ring, an all planar structure is

feasible. This is found in a recent structure of $((CH_3)_2$-$P(CH_2)_2)_2Au_2Cl_2$.[22d]

Why do these d^9 dimers avoid the alternative bridging geometry **56**? To probe this question we studied a model tetra-

56
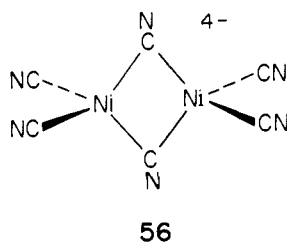
hedral dimer **56**. Its energy came out 1.2 eV above the observed structure. More important, there was a minute gap of 0.06 eV between the filled and unfilled levels. The tetrahedral dimer would be a high spin complex or would be subject to a second-order Jahn–Teller distortion.

The level pattern in **56** is quite different from that of the other d^9 tetrahedral dimers which we have studied earlier. The $2b_{1u}$ level, which in Figure 5 could be seen clearly isolated as the highest d band orbital, in $Ni_2(CN)_6^{4-}$ finds a place in the middle of the band. It is depressed in energy by interaction with the relatively low-lying π^* acceptor orbitals of the bridging cyanides—in contrast to in-plane donation in the chloro and phosphido bridged cases discussed earlier. In general the terminal and bridging cyanide π^* levels keep any of the d levels from rising too high and forming a well-defined gap between filled and unfilled levels. We think a similar effect pushes $(PPh_3)_2Rh(CO)_2Rh(PPh_3)_2$ away from an idealized tetrahedral dimer structure and toward the most interesting geometry that it does assume.[21] In general we expect $X_2MY_2MX_2$ species with $Y = \pi$-acceptor to avoid the tetrahedral dimer structure.

While we have examined a number of geometrical extremes, it is clear that our job is far from complete. For instance we have avoided discussion of the pathways interconverting the $Ni_2(CN)_6^{4-}$ type dimers with their tetrahedral and square planar counterparts, as well as the possible processes interchanging sites in all these species. We have not discussed the ethane type structures, represented by $(PPh_3)(NO)_2Ir$-$Ir(NO)_2(PPh_3)$[49] or the triply bonded $Mo_2(CH_2SiMe_3)_6$,[50] $Mo_2(NMe_2)_6$,[51] and $W_2(NMe_2)_6$.[52] These are problems for the future.

The conclusions we come to have been stated in the introductory paragraph of this paper. The geometrical and electronic structure of these tetrahedral dimers is set by three factors: the geometrical preference of the monomer, the differential through-bond coupling, and direct metal–metal bonding. While our simultaneous analysis of all three factors may have been involved, it has led us to a better understanding of the dimers as well as some interesting sidelights on the geometry of d^{10} MX_2Y_2 complexes and the choice between tetrahedral and square planar dimers.

Appendix 1

Bending of Nitrosyl Groups in Tetrahedral Dinitrosyl Complexes. In tetrahedral dinitrosyl complexes the M–N–O angles often depart by moderate amounts from 180°. Thus in
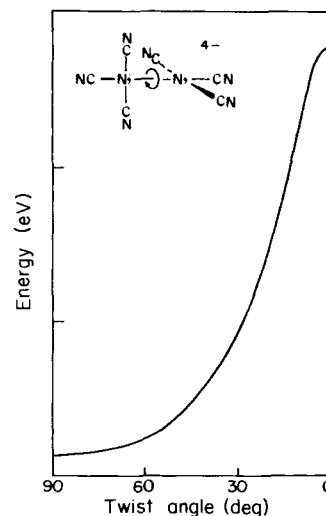
Figure 12. Total energy as a function of twist angle in $Ni_2(CN)_6^{4-}$. The energy scale markings are 1 eV apart.

8 the N–Co–N angle is 118° and the nitrosyls are bent toward each other, with a Co–N–O angle $\sim$170°.[2j] In $(Ph_3P)_2$-$Rh(NO)_2^+$ the N–Rh–N angle is 157.5° and the nitrosyls are bent away from each other with an Rh–N–O angle of 159°.[37g] In the intermediate case **34** with an N–Os–N angle of 139° the bending is less, with an average Os–N–O angle of 177° bent away.[37a] Though the extent of bending in these cases is considerably less than in the strongly bent nitrosyls, the variable direction of bending is interesting and has received some attention.[37,40,41,53] The degree and direction of this bending can be explained quite easily as a secondary function of the N–M–N angle. The angle between the nitrosyls is set by the factors we have already discussed; that is, the better the possible π bonding with the metal donor orbitals the wider will be the N–M–N angle.

Once the general magnitude of the N–M–N angle is established, it is possible to talk about the bending of the nitrosyls. Two metal orbitals are most affected by this bending motion, **57** and **58**. Orbital **57**, of b_1 symmetry in C_{2v}, is de-

57

58
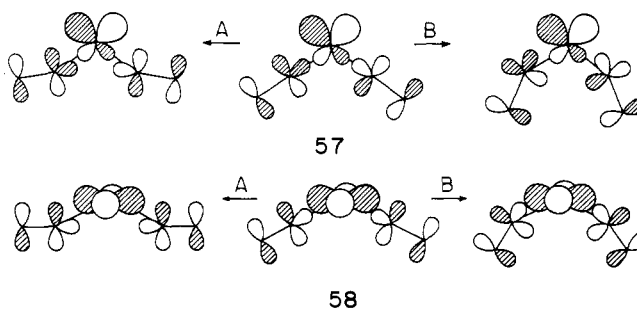
stabilized by the ligand lone pair at acute N–M–N angles. Distortion A, bending the nitrosyls away from each other, enhances this repulsion by placing the lone pair density at an effectively smaller angle. The NO π^* orbitals are not effective in stabilizing this distortion because the N p orbital density will be near the node of the metal d–p hybrid. Distortion B, on the other hand, places the NO lone pair on the node of the metal orbital and allows the NO π^* to stabilize the metal orbital. Thus interactions with orbital **57** favor distortion B, bending the nitrosyls toward each other.

Interactions with the a_1, predominately $x^2 - y^2$, orbital **58**, however, favor distortion A. As the nitrosyls bend apart, the NO lone pair–metal d antibonding overlap decreases, and the π^* orbitals become more metal–nitrosyl bonding. In distortion B this orbital is pushed up by increased repulsions between the

Table III. Bending Preference of Nitrosyls in $Co(H)_2(NO)_2^-$ as a Function of N-Co-N Angle

N-Co-N[a] $\theta°$	Co-N-O[a] $\phi°$
110	169
130	179
150	188

[a] The angles are defined in **59**.

Table IV. Metal 4s and 4p Exponents Which Give Reasonable Calculated Metal-Metal Bond Distances

| Compound	Metal ζ 4s, 4p	M-M, Å Calcd	M-M, Å Exptl
$Cr_2(CO)_{10}^{2-}$	1.7	2.99	2.97[a]
$Mn_2(CO)_{10}$	1.8	2.93	2.92[b]
$Fe_2(CO)_8^{2-}$	1.9	2.80	2.79[c]
$Co_2(CO)_8$	2.0	2.67	2.66[d]

[a] Reference 2n. [b] L. F. Dahl and R. E. Rundle, *Acta Crystallogr.*, **16**, 419 (1963). [c] H. B. Chin, M. B. Smith, R. D. Wilson, and R. Bau, *J. Am. Chem. Soc.*, **96**, 5285 (1974). [d] The Co-Co distance in (n-Bu$_3$P)$_2$Co$_2$(CO)$_6$: J. A. Ibers, *J. Organomet. Chem.*, **14**, 423 (1968).

lone pair and metal while the ligand acceptor orbitals remain ineffective.

The result of distortion is thus in opposite directions for **57** and **58**. Which one dominates depends on the N-M-N angle. The distortion causes the greatest stabilization when it occurs in the most antibonding situation. **57** has a greater slope at low N-M-N angle, **58** for a more open ON-M-NO grouping. Thus stabilization of **57** through distortion B predominates at low N-M-N angles. At large N-M-N angles, stabilization of **58** through distortion A is most important. A sample calculation on $(ON)_2CoH_2^-$, **59**, shows these effects (Table III).
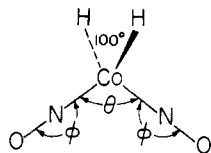
59

For another rationalization of the dinitrosyl distortions the reader is directed to the work of Enemark and Feltham.[41]

Appendix 2

Computational Details. All the calculations were of the extended Hückel type.[54] Parameters used previously[54] for carbon, nitrogen, oxygen, and hydrogen were kept fixed during all charge iterations. Exponents for the 3s and 3p orbitals of chlorine and phosphorus were calculated from Burns' rules.[55] Exponents for the 5s and 5p orbitals of iodine are from the work of Clementi and Roetti.[56] For metals of the first transition series 3d orbital exponents for the +1 ions were taken from the work of Richardson et al.[57] For second-row metals 4d, 5s, and 5p exponents are those determined by Basch and Gray.[58]

It has been noted[59] that the available 4s and 4p exponents for the first transition series[55,57,60] are small compared to the corresponding parameters for the second- and third-row metals.[58] Increasing the exponents for the first-row metals leads to a larger interaction with ligand σ orbitals and generally better computational results.[59,61] In particular the diffuse metal s and p orbitals we have used previously result in small negative metal-metal overlap populations in transition metal

Table V. Extended Hückel Parameters

Orbital	H_{ii} eV	Exponents[a] ζ_1	Exponents[a] ζ_2
H 1s	−13.6	1.3	
C 2s	−21.4	1.625	
C 2p	−11.4	1.625	
N 2s	−26.0	1.950	
N 2p	−13.4	1.950	
O 2s	−32.3	2.275	
O 2p	−14.8	2.275	
P 3s	−18.6	1.75	
P 3p	−14.0	1.30	
Cl 3s	−26.3	2.183	
Cl 3p	−14.2	1.733	
I 5s	−23.3	2.681	
I 5p	−14.0	2.322	
Cr 4s	−8.66	1.7	
Cr 4p	−5.24	1.7	
Cr 3d	−11.2	4.95 (0.5060)	1.80 (0.6750)
Mn 4s	−9.75	1.8	
Mn 4p	−5.89	1.8	
Mn 3d	−11.67	5.15 (0.5320)	1.90 (0.6490)
Fe 4s	−9.10	1.9	
Fe 4p	−5.32	1.9	
Fe 3d	−12.6	5.35 (0.5505)	2.00 (0.6260)
Co 4s	−9.21	2.0	
Co 4p	−5.29	2.0	
Co 3d	−13.18	5.55 (0.5680)	2.10 (0.6060)
Ni 4s	−10.95	2.1	
Ni 4p	−6.27	2.1	
Ni 3d	−14.2	5.75 (0.5798)	2.30 (0.5782)
Cu 4s	−11.4	2.2	
Cu 4p	−6.06	2.2	
Cu 3d	−14.0	5.95 (0.5933)	2.30 (0.5744)
Nb 5s	−10.1	1.89	
Nb 5p	−6.86	1.85	
Nb 4d	−12.1	4.08 (0.6401)	1.64 (0.5516)
Mo 5s	−8.34	1.96	
Mo 5p	−5.24	1.90	
Mo 4d	−10.50	4.54 (0.6097)	1.90 (0.6097)
Rh 5s	−8.09	2.135	
Rh 5p	−4.57	2.10	
Rh 4d	−12.5	4.29 (0.5807)	1.97 (0.5685)
Pt 6s	−9.077	2.554	
Pt 6p	−5.475	2.554	
Pt 5d	−12.59	6.013 (0.6334)	2.696 (0.5513)

[a] Two Slater exponents are listed for the 3d functions. Each is followed in parentheses by the coefficient in the double zeta expansion.

dimers, even in complexes such as $Fe_2(CO)_8^{2-}$ which have obvious metal-metal bonds. We have adjusted the metal 4s and 4p exponents to give proper metal-metal distances in dimers with unsupported metal-metal bonds. Except for the metal-metal distance the experimental geometries were maintained throughout these calculations. The exponents of the s and p orbitals were assumed to be equal for a given metal. To emphasize the approximate nature of these parameters they are estimated only to two places in Table IV. In order to check the behavior of the parameters of Basch and Gray[58] for the heavier metals the Mo-Mo bond length in $Mo_2(CO)_{10}^{2-}$ ^{2n} was calculated using those exponents. The calculated Mo-Mo distance was 3.11, the experimental 3.13 Å.[2ll]

The exponents for metal 4s and 4p orbitals listed in Table IV are now more in line with the parameters for the heavier metals[58] which also seem to give reasonable metal-metal bond lengths. In addition these new 4s and 4p functions are similar to those determined by the Fenske group from maximum overlap criteria.[2w,59,62]

Metal H_{ii}'s for Cr,[63] Mn,[17d] Ni,[64] Cu,[1b] and Pt[65] were taken from other work. For Fe, Co, Nb, and Rh charge iterations were performed on suitable model compounds ($Fe_2(NO)_4I_2$, $Co_2(NO)_4Cl_2$, $Nb_2(CH_3)_4(CH)_2$, and $Rh(CO)_2Cl_2^-$) assuming a quadratic dependence of metal H_{ii}'s on charge.[66] In the iodide bridged dimer the iodine H_{ii}'s were assumed to vary in a linear way with charge with a slope of 7.9 eV/e from neutral atom VSOIP's of 21.0 eV for the 5s and −10.45 eV for the 5p orbitals. A linear dependence was also assumed for the chlorine H_{ii}'s in $Co_2(NO)_4Cl_2$ with a slope of 10.66 eV/e from neutral atom VSOIP's of −25.9 eV for the 3s and −13.8 eV for the 3p orbitals. In the iteration on $Rh(CO)_2Cl_2^-$ the Cl H_{ii}'s were fixed at −27.5 eV for the 3s and −17.4 eV for the 3p orbitals. All geometrical deformations were examined by extended Hückel calculations without charge iteration using the parameters obtained from these models. These are collected in Table V.

References and Notes

(1) (a) R. Hoffmann, *Acc. Chem. Res.*, **4**, 1 (1971); (b) P. J. Hay, J. C. Thibeault, and R. Hoffmann, *J. Am. Chem. Soc.*, **97**, 4884 (1975).
(2) (a) L. F. Dahl and D. L. Wampler, *Acta Crystallogr.*, **15**, 903 (1962); *J. Am. Chem. Soc.*, **81**, 3150 (1959); (b) L. F. Dahl, C. Martell, and D. L. Wampler, *ibid.*, **83**, 1761 (1961); (c) L. F. Dahl and P. W. Sutton, *Inorg. Chem.*, **2**, 328 (1963); (d) L. F. Dahl and C.-H. Wei, *Inorg. Chem.*, **2**, 328 (1963); C. H. Wei and L. F. Dahl, *ibid.*, **4**, 1, 493 (1965); **6**, 1229 (1967); **9**, 1878 (1970); *J. Am. Chem. Soc.*, **90**, 3960, 3969, 3977, (1969); (e) L. F. Dahl and J. F. Blount, *Inorg. Chem.*, **4**, 1373 (1965); (f) J. F. Blount, L. F. Dahl, C. Hoogzand, and W. Hübel, *J. Am. Chem. Soc.*, **88**, 292 (1966); (g) J. M. Coleman and L. F. Dahl, *ibid.*, **89**, 543 (1967); (h) D. L. Stevenson and L. F. Dahl, *ibid.*, **89**, 3721 (1967); (i) L. F. Dahl, W. R. Costello, and R. B. King, *ibid.*, **90**, 5422 (1968); (j) L. F. Dahl, E. Rodulfo de Gil, and R. D. Feltham, *ibid.*, **91**, 1653 (1969); (k) R. Vranka, L. F. Dahl, P. Chini, and J. Chatt, *ibid.*, **91**, 1574 (1969); (l) C. E. Strouse and L. F. Dahl, *Discuss. Faraday Soc.*, **47**, 93 (1969); *J. Am. Chem. Soc.*, **93**, 6032 (1971); (m) A. S. Foust, M. S. Foster, and L. F. Dahl, *ibid.*, **91**, 5631, 5633 (1969); (n) L. B. Handy, J. K. Ruff, and L. F. Dahl, *ibid.*, **92**, 7312, 7327 (1970); (o) A. S. Foust and L. F. Dahl, *ibid.*, **92**, 7337 (1970); (p) N. G. Connelly and L. F. Dahl, *ibid.*, **92**, 7470, 7472 (1970); (q) J. K. Ruff, R. P. White, Jr., and L. F. Dahl, *ibid.*, **93**, 2159 (1971); (r) Trinh-Toan, W. P. Fehlhammer, and L. F. Dahl, *ibid.*, **94**, 3389 (1972); (s) G. L. Simon and L. F. Dahl, *ibid.*, **95**, 783, 2164, 2175 (1973); (t) C. H. Wei, L. Markó, G. Bor, and L. F. Dahl, *ibid.*, **95**, 4840 (1973); (u) B. K. Teo, M. B. Hall, R. F. Fenske, and L. F. Dahl, *J. Organomet. Chem.*, **70**, 413 (1974); (v) R. S. Gull, N. G. Connelly, and L. F. Dahl, *J. Am. Chem. Soc.*, **96**, 4017 (1974); R. S. Gall, C. T.-W. Chu, and L. F. Dahl, *ibid.*, **96**, 4019 (1974); (w) B. K. Teo, M. B. Hall, R. F. Fenske, and L. F. Dahl, *Inorg. Chem.*, **14**, 3103 (1975).
(3) F. A. Cotton and D. A. Ucko, *Inorg. Chim. Acta*, **6**, 161 (1972), and references therein; F. A. Cotton, *Pure Appl. Chem.*, **17**, 25 (1967).
(4) R. Mason and D. M. P. Mingos, *J. Organomet. Chem.*, **50**, 53 (1973).
(5) Among numerous reference see the following: (a) J. Lewis, *Pure Appl. Chem.*, **10**, 11 (1965); (b) A. P. Ginsberg and E. Koubek, *Inorg. Chem.*, **4**, 1517 (1965).
(6) (a) D. G. Sekutowski and G. D. Stucky, *Inorg. Chem.*, **14**, 2192 (1975); (b) S. C. Wallwork and I. J. Worrall, *J. Chem. Soc.*, **1816** (1965).
(7) Additional structures exhibiting this elongation are: (a) [Br(PEt₃)CdBr]₂ and [Br(AsBu₃)HgBr]₂: R. C. Evans, F. G. Mann, H. S. Peiser, and D. Purdie, *J. Chem. Soc.*, 1209 (1940); (b) [(1,5-cyclooctadiene)CuCl]₂: J. H. van den Hende and W. C. Baird, Jr., *J. Am. Chem. Soc.*, **85**, 1009 (1963); (c) {[Cp(CO)₃Mo][Et₂O]ZnCl}₂: J. St. Denis, W. Botler, M. D. Glick, and J. P. Oliver, *ibid.*, **96**, 5427 (1974); (d) (PPh₃)₄Ag₂Br₂: B.-K. Teo and J. C. Calabrese, *J. Chem. Soc., Chem. Commun.*, 185 (1976).
(8) For an analysis of these ring systems that emphasizes Cl–Cl nonbonded forces see F. K. Ross and G. D. Stucky, *J. Am. Chem. Soc.*, **92**, 4538 (1970).
(9) (a) R. Graziani, G. Bombieri, and E. Forsellini, *J. Chem. Soc. A*, 2331 (1971); (b) S. Htoon and M. F. C. Ladd, *J. Cryst. Mol. Struct.*, **3**, 95 (1973).
(10) S. Jagner and N.-G. Vannerberg, *Acta Chem. Scand.*, **21**, 1183 (1967).
(11) For a similar effect in another d¹⁰ system, Cu(I), one can compare the 73° angle at bridging S in Cu₂(thiourea)₆²⁺: I. F. Taylor, Jr., M. S. Weininger, and E. L. Amma, *Inorg. Chem.*, **13**, 2835 (1974), with the corresponding 83° angle in the infinite chain structure of Cu(thiourea)₂Cl: W. A. Spofford, III, and E. L. Amma, *Acta Crystallogr., Sect. B*, **26**, 1474 (1970).
(12) J. T. Thomas, J. H. Robertson, and E. G. Cox, *Acta Crystallogr.*, **11**, 604 (1958).
(13) W. Clegg (private communication). We are grateful to J. K. Burdett for bringing this work to our attention.
(14) J. A. J. Jarvis, R. H. B. Mais, P. G. Owston, and D. T. Thompson, *J. Chem. Soc. A*, 1867 (1970).
(15) In the structures which contain nitrosyl groups there is a variable degree of M–N–O bending from 180°.
(16) For CuCl₄²⁻ structures see: (a) R. L. Harlow, W. J. Wells, III, G. W. Watt, and S. H. Simonsen, *Inorg. Chem.*, **13**, 2106 (1974); (b) J. Lamotte-Brasseur, O. Dideberg, and L. Dupont, *Cryst. Struct. Commun.*, **1**, 313 (1972); (c) R. D. Willett and M. L. Larsen, *Inorg. Chim. Acta*, **5**, 175 (1971); (d) M. Bonamico, G. Dessy, and A. Vaciago, *Theor. Chim. Acta*, **7**, 367 (1967); (e) R. Clay, J. Murray-Rust, and P. Murray-Rust, *Acta Crystallogr., Sect. B*,

31, 289 (1975); (f) see "Molecular Structure by Diffraction Methods", Vol. 1, Specialist Periodical Report of the Chemical Society, London, 1973, p 642.
(17) For calculations on this and related d⁹ monomers see (a) L. L. Lohr, Jr., and W. N. Lipscomb, *Inorg. Chem.*, **2**, 911 (1963); (b) C. J. Ballhausen, N. Bjerrum, R. Dingle, K. Eriks and C. R. Hare, *ibid.*, **4**, 514 (1965); (c) J. Demuynck, A. Veillard, and U. Wahlgren, *J. Am. Chem. Soc.*, **95**, 5563 (1973); (d) M. Elian and R. Hoffmann, *Inorg. Chem.*, **14**, 1058 (1975); (e) J. K. Burdett, *J. Chem. Soc., Faraday Trans.2*, **70**, 1599 (1974); *Inorg. Chem.*, **14**, 375 (1975).
(18) (a) S. C. Abrahams and H. J. Williams, *J. Chem. Phys.*, **39**, 2923 (1963); (b) P. H. Vossos, D. R. Fitzwater, and R. E. Rundle, *Acta Crystallogr.*, **16**, 1037 (1963); (c) R. D. Willett, C. Dwiggins, Jr., R. T. Kruh, and R. E. Rundle, *J. Chem. Phys.*, **38**, 2429 (1963); (d) R. D. Willett, *ibid.*, **44**, 39 (1966); (e) *J. Chem. Soc., Chem. Commun.*, 607 (1973); (f) R. D. Willett and C. Chow, *Acta Crystallogr., Sect. B*, **30**, 207 (1974); (g) for some related Cl bridged Cu(II) structures see R. D. Willett and R. E. Rundle, *J. Chem. Phys.*, **40**, 838 (1962).
(19) (a) Reviewed by D. J. Hodgson, *Prog. Inorg. Chem.*, **19**, 173 (1975); (b) see ref 16f, p 674.
(20) B. L. Barnett, C. Krüger, and Y.-H. Tsay, cited in P. W. Jolly and G. Wilke "The Organic Chemistry of Nickel", Vol. 1, Academic Press, New York, N.Y., 1974, p 145. See also C. Krüger, *Angew. Chem.*, **84**, 412 (1972). The compound was synthesized by K. Jonas and G. Wilke, *ibid.*, **82**, 295 (1970).
(21) P. Singh, C. B. Damman, and D. J. Hodgson, *Inorg. Chem.*, **12**, 1335 (1973). Synthesis: D. Evans, G. Yagupsky, and G. Wilkinson, *J. Chem. Soc. A*, 2660 (1968).
(22) (a) O. Jarchow, *Z. Anorg. Allg. Chem.*, **383**, 40 (1971); *Z. Kristallogr., Kristallgeom. Kristallphys., Kristallchem.*, **136**, 122 (1973); O. Jarchow, H. Schulz, and R. Nast, *Angew. Chem.*, **82**, 43 (1970); (b) A. Modinos and P. Woodward, *J. Chem. Soc., Dalton Trans.*, 1516 (1975), determine the structure of one of two modifications reported by P. L. Goggin and R. J. Goodfellow, *ibid.*, 2355 (1973); (c) D. J. Doonan, A. L. Balch, S. Z. Goldberg, R. Eisenberg, and J. S. Miller, *J. Am. Chem. Soc.*, **97**, 1961 (1975); S. Z. Goldberg and R. Eisenberg, *Inorg. Chem.*, **15**, 535 (1976); (d) H. Schmidbaur, J. R. Mandl, A. Frank, and G. Huttner, *Chem. Ber.*, **109**, 466 (1976).
(23) J. Reed, A. J. Schultz, C. G. Pierpont, and R. Eisenberg, *Inorg. Chem.*, **12**, 2949 (1973).
(24) R. Mason, I. Sotofte, S. D. Robinson, and M. F. Uttley, *J. Organomet. Chem.*, **46**, C61 (1972).
(25) (a) K. Nicholas, L. S. Bray, R. E. Davis, and R. Pettit, *Chem. Commun.*, 608 (1971); (b) a related 3,3,6,6-tetramethyl-1-thiacycloheptyne complex was determined by H. J. Schmitt and M. L. Ziegler, *Z. Naturforsch. B*, **28**, 508 (1973).
(26) We note incidentally that (NO)(PPh₃)Ir(CF₃C₂CF₃)₂Ir(NO)(PPh₃), which, if we consider the acetylene ligands as neutral and the nitrosyls as NO⁺ has two more electrons per metal atom, assumes a very different diiridiacyclohexadiene geometry: J. Clemens, M. Green, M.-C. Kuo, C. J. Fritchie, Jr., J. T. Mague, and F. G. A. Stone, *J. Chem. Soc., Chem. Commun.*, 53, (1972).
(27) D. R. Russell, P. A. Tucker, and C. Whittaker, *Acta Crystallogr., Sect. B*, **31**, 2530 (1975); N. C. Stephenson, *Acta Crystallogr.*, **17**, 587 (1964).
(28) For each entry we indicate the metal and the bridging group. (a) Ni(II), SEt: P. Woodward, L. F. Dahl, E. W. Abel, and B. C. Crosse, *J. Am. Chem. Soc.*, **87**, 5251 (1965); (b) Ni(II) and Pd(II), SC₂H₄OH: R. O. Gould and M. M. Harding, *J. Chem. Soc. A*, 875 (1970); (c) Ni(II), SR: D. J. Baker, D. C. Goodall, and D. S. Moss, *Chem. Commun.*, 325 (1969); (d) Ni(II), SEt: A. Chiesi Villa, A. Gaetani Manfredotti, M. Nardelli, and C. Pelizzi, *Chem. Commun.*, 1322 (1970); (e) Ni(II), SCH₂Ph and Pd(II), S-*tert*-butyl: J. P. Fackler, Jr., and W. J. Zegarski, *J. Am. Chem. Soc.*, **95**, 8566 (1973); (f) Rh(I), Cl: K. A. Klanderman, *Diss. Abstr.*, **25**, 6253 (1965); (g) RH(I), Cl: J. Coetzer and G. Gafner, *Acta Crystallogr., Sect. B*, **26**, 985 (1970); (h) Rh(I), Cl: M. G. B. Drew, S. M. Nelson, and M. Sloan, *J. Chem. Soc., Dalton Trans.*, 1484 (1973); (i) Rh(I), Cl: J. J. Bonnet, Y. Jeannin, P. Kalck, A. Maisonnat, and R. Poilblanc, *Inorg. Chem.*, **14**, 743 (1975); (j) Pd(II), SPr: N. R. Kunchur, *Acta Crystallogr., Sect. B*, **24**, 1623 (1968); (k) Pd(II), Cl: G. R. Davies, R. H. B. Mais, S. O'Brien, and P. G. Owston, *Chem. Commun.*, 1151 (1967); (l) Pd(II), Cl: J. Lukas, J. E. Ramakers-Blom, T. G. Hewitt, and J. J. deBoer, *J. Organomet. Chem.*, **46**, 167 (1972); (m) Pd(II), Br: B. J. Kilbourn, R. H. B. Mais, and P. G. Owston, *Chem. Commun.*, 1438 (1968); (n) Pt(II), allyl and Cl: G. Raper and W. S. McDonald, *J. Chem. Soc., Dalton Trans.*, 265 (1972); (o) Pt(II), SEt: M. C. Hall, J. J. Jarvis, B. T. Kilbourn, and P. G. Owston, *ibid.*, 1544 (1972).
(29) For each entry we indicate the metal atom and the nature of the bridging group. (a) Ni(II), Br: M. R. Churchill and T. A. O'Brien, *Inorg. Chem.*, **6**, 1386 (1967); (b) Rh(I), Cl: J. A. Ibers and R. G. Snyder, *J. Am. Chem. Soc.*, **84**, 495 (1962); (c) Pd(II), C₆F₅S: R. H. Fenn and G. R. Segrott, *J. Chem. Soc. A*, 3197 (1970); (d) Pd(II), Cl: J. N. Dempsey and N. C. Baenziger, *J. Am. Chem. Soc.*, **77**, 4984 (1955); (e) Pd(II), Cl: J. R. Holden and N. C. Baenziger, *ibid.*, **77**, 4987 (1955); (f) Pd(II), Cl: W. E. Oberhansli and L. F. Dahl, *J. Organomet. Chem.*, **3**, 43 (1965); A. E. Smith, *Acta Crystallogr.*, **18**, 331 (1965); (g) Pd(II), Cl: W. E. Oberhansli and L. F. Dahl, *Inorg. Chem.*, **4**, 629 (1965); (h) Pd(II), Cl: M. Kh. Minasian, S. P. Gubin, and Yu. T. Struchkov, *Zh. Strukt. Khim.*, **8**, 1108 (1967); (i) Pd(II), Cl: R. Mason and A. G. Wheeler, *Nature (London)*, **217**, 1253 (1968); (j) Pd(II), Cl: K. Oda, N. Yasuoka, T. Veki, N. Kasai, and M. Kakudo, *Bull. Chem. Soc. Jpn.*, **43**, 362 (1970); (k) Pd(II), Cl: F. Dahan, C. Agami, J. Levisalles, and F. Rose-Munch, *J. Chem. Soc., Chem. Commun.*, 505 (1974); (l) Pd(II), Br: F. G. Mann and A. F. Wells, *J. Chem. Soc.*, 702 (1938); (m) Pd(II), Br and Pt(II), SEt₂: D. L. Sales, J. Stokes, and P. Woodward, *J. Chem. Soc. A*, 1852 (1968); (n) Pd(II), I: G. Thiele, K. Brodersen, E. Kruse, and B. Holle, *Chem. Ber.*, **101**, 2771 (1968); (o) Pt(II), NH₂ and N₂H: G. C. Dobinson, R. Mason, G. R. Robertson, R. Ugo, F. Conti, D. Morelli, S. Cenini, and F. Bonati, *Chem. Commun.*, 739 (1967); (p) Pt(II), Cl: W. A. Whitla, H. M. Powell, and L. M. Venanzi, *ibid.*, 310 (1966); (q) Pt(II),

7254

Cl: M. Black, R. H. B. Mais, and P. G. Owston, *Acta Crystallogr., Sect B*, **25**, 1760 (1969); (r) Pt(II), Cl: S. F. Watkins, *J. Chem. Soc. A*, 168 (1970); (s) Au(III), Br: S. Burawoy, C. S. Gibson, G. C. Hampson, and H. M. Powell, *J. Chem. Soc.*, 1690 (1937); (t) Au(III), Cl: E. S. Clark, D. H. Templeton, and C. MacGillavry, *Acta Crystallogr.*, **11**, 284 (1958).

(30) W. Harrison, N. L. Paddock, J. Trotter, and J. N. Wingfield, *J. Chem. Soc., Chem. Commun.*, 23 (1972); W. Harrison and J. Trotter, *J. Chem. Soc., Dalton Trans.*, 61 (1973).

(31) C. L. Raston and A. H. White, *J. Chem. Soc., Dalton Trans.*, 2410 (1975).

(32) (a) O. Hassel, *Acta Chem. Scand.*, **1**, 149 (1947); (b) E. Z. Zasorin, N. G. Rambidl, and P. A. Akishin, *Zh. Strukt. Khim.*, **4**, 910 (1963); (c) apparently present in solution in this form as well: D. L. Wertz and R. F. Kruh, *J. Chem. Phys.*, **50**, 4013 (1969).

(33) J. J. Mayerle, R. B. Frankel, R. H. Holm, J. A. Ibers, W. D. Phillips, and J. F. Weiker, *Proc. Natl. Acad. Sci. U.S.A.*, **70**, 2429 (1973); J. J. Mayerle, S. E. Denmark, B. V. DePamphilis, J. A. Ibers, and R. H. Holm, *J. Am. Chem. Soc.*, **97**, 1032 (1975); W. O. Gillum, R. B. Frankel, S. Foner, and R. H. Holm, to be submitted for publication.

(34) (a) W. Mowat and G. Wilkinson, *J. Chem. Soc., Dalton Trans.*, 1120 (1973); (b) F. Huq, W. Mowat, A. C. Skapski, and G. Wilkinson, *Chem. Commun.*, 1477 (1971).

(35) Throughout this paper we use the abbreviations s, x, y, z, xz, yz, z^2, $x^2 - y^2$, xy for the corresponding metal ns, np, and $(n-1)d$ orbitals.

(36) The iodide was calculated with an M–N–O angle of 160°, to simulate the experimental dimer structure (ref 2j). In the chloride an M–N–O angle of 170° was used, as observed in the dimer (ref 10).

(37) (a) (PPh₃)₂Os(NO)₂, N–Os–N = 139°, P–Os–P = 103.5°: B. L. Haymore and J. A. Ibers, *Inorg. Chem.*, **14**, 2610 (1975); (b) (PPh₃)₂Ru(NO)₂, N–Ru–N 139°, P–Ru–P 104°: A. P. Gaughan, Jr., B. J. Corden, R. Eisenberg, and J. A. Ibers, *ibid.*, **13**, 786 (1974); S. Bhaduri and G. M. Sheldrick, *Acta Crystallogr., Sect. B*, **31**, 897 (1975); (c) (PPh₃)₂Fe(NO)₂, N–Fe–N 124°, P–Fe–P 112°: V. G. Albano, A. Araneo, P. L. Bellon, G. Ciani, and M. Manassero, *J. Organomet. Chem.*, **67**, 413 (1974); (d) (PPh₃)₂Ir(NO)₂⁺, N–Ir–N 154°, P–Ir–P 116°: D. M. P. Mingos and J. A. Ibers, *Inorg. Chem.*, **9**, 1105 (1970); (e) (f₆fos)Fe(NO)₂, N–Fe–N 125°, P–Fe–P 87°: W. Harrison and J. Trotter, *J. Chem. Soc. A*, 1542 (1971) (in this case the cyclic diphosphine is constrained); (f) Co(NO)₂(PPh₂(CH₂)₂PPh₂O)I, N–Co–N = 120°, P–Co–I = 97°: J. S. Field, P. J. Wheatley, and S. Bhaduri, *J. Chem. Soc., Dalton Trans.*, 74 (1974); (g) (Ph₃P)₂Rh(NO)₂⁺, N–Rh–N 157.5°, P–Rh–P 115.9°: J. A. Kaduk and J. A. Ibers, *Inorg. Chem.*, **14**, 3070 (1975); (h) (np₂O)-Co(NO)₂⁺: C. A. Ghilardi and L. Sacconi, *Cryst. Struct. Commun.*, **4**, 687 (1975).

(38) (a) V. G. Albano, P. L. Bellon, and M. Sansoni, *J. Chem. Soc. A*, 2420 (1971); (b) (PPh₂Et)₂Pt(CO)₂, C–Pt–C 117°, P–Pt–P 98°: V. G. Albano, P. L. Bellon, and M. Manassero, *J. Organomet. Chem.*, **35**, 423 (1972); (c) (Me₂NNC(Me)C(Me)NNMe₂)Ni(CO)₂, a constrained cyclic ligand, C–Ni–C 105°, N–Ni–N 81°: H. D. Hausen and K. Krogmann, *Z. Anorg. Allg. Chem.*, **389**, 247 (1972); (d) a case that does not appear to fit our generalization is (PPh₃)₂Ni(CO)₂, C–Ni–C 113°, P–Ni–P 117° C. Krüger and Y.-H. Tsay, *Cryst. Struct. Commun.*, **3**, 455 (1974).

(39) (a) (PPh₃)₂Ir(CO)(NO), C–Ir–N 129°, P–Ir–P 104°: C. P. Brock and J. A. Ibers, *Inorg. Chem.*, **11**, 2812 (1972); (b) (PPh₃)₂Co(CO)(NO), C–Co–N 120°, P–Ir–P 114°: V. G. Albano, P. L. Bellon, and G. Ciani, *J. Organomet. Chem.*, **38**, 155 (1972).

(40) A case with azide and nitrosyl substitution that fits this pattern as well is (PPh₃)₂Ni(N₃(NO) studied by J. H. Enemark, *Inorg. Chem.*, **10**, 1952 (1971).

(41) A theoretical account of distortions in dinitrosyls is given by J. H. Enemark and R. D. Feltham, *Coord. Chem. Rev.*, **13**, 339 (1974).

(42) Structures summarized by S. J. Lippard and G. J. Palenik, *Inorg. Chem.*,

(10, 1322 (1971), and F. H. Jardine, *Adv. Inorg. Chem. Radiochem.*, **17**, 115 (1975).

(43) Our analysis of the factors influencing distortions in X₂MY₂ d¹⁰ complexes is not complete, for there are some structures in which the observed distortions do not fit the anticipated pattern. For instance, in Cl₂Hg(OAsPh₃)₂ the Cl–Hg–Cl angle is significantly opened to 146.6°, while O–Hg–O is 92.5°: C. I. Brändén, *Acta Chem. Scand.*, **17**, 1363 (1963). On the other hand, still other Hg(II) structures show angles close to tetrahedral: K. Aurivillius and L. Fälth, *Chem. Scr.*, **4**, 215 (1973); L. Fälth, *ibid.*, **9**, 71 (1976).

(44) Throughout this discussion we assume that in X₂MY₂ complexes the distortion keeps the X–M–X and Y–M–Y planes orthogonal. This is not necessarily so, either in dimers (see ref 19, 20, 21) nor in monomers; see the structure of Cl₂Cu(OPPh₃)₂: J. A. Bertrand and A. R. Kalyanaraman, *Inorg. Chim. Acta*, **5**, 341 (1971).

(45) (a) J. A. J. Jarvis, R. H. B. Mais, and P. G. Owston, *J. Chem. Soc. A*, 1473 (1968); (b) (PPh₃)₂NiCl₂, Cl–Ni–Cl 123°, P–Ni–P 117°: G. Garton, D. E. Henn, H. M. Powell, and L. M. Venanzi, *J. Chem. Soc.*, 3625 (1963); (c) [PPh₂(CH₂Ph)]₂NiBr₂, Br–Ni–Br 120°, P–Ni–P 105°: B. T. Kilbourn and H. M. Powell, *J. Chem. Soc. A*, 1688 (1970). This is the remarkable structure with both high-spin tetrahedral and low-spin square planar Ni(II) in the same solid state structure. (d) Two constrained systems with one cyclic ligand and NiX₂ possible show this effect: P. T. Greene and L. Sacconi, *J. Chem. Soc. A*, 866 (1970); D. L. Johnston, W. L. Rohrbaugh, and W. de W. Horrocks, Jr., *Inorg. Chem.*, **10**, 547 (1971).

(46) J. K. Burdett, Newcastle upon Tyne, to be submitted for publication.

(47) For other calculations on square-planar dimers, see (a) V. I. Baranovskii, M. K. Davydova, N. S. Panina, and A. I. Panin, *Koordin. Khim.*, **2**, 409 (1976); (b) D. S. Martin, Jr., R. M. Rush, and T. J. Peters, *Inorg. Chem.*, **15**, 669 (1976).

(48) See the discussion by R. Poilblanc, *J. Organomet. Chem.*, **94**, 241 (1975).

(49) M. Angoletta, G. Ciani, M. Manassero, and M. Sansoni, *J. Chem. Soc., Chem. Commun.*, 789 (1973).

(50) F. Huq, W. Mowat, A. Shortland, A. C. Skapski, and G. Wilkinson, *Chem. Commun.*, 1079 (1971).

(51) M. Chisholm, F. A. Cotton, B. A. Frenz, and L. Shive, *J. Chem. Soc., Chem. Commun.*, 480 (1974).

(52) F. A. Cotton, B. R. Stults, J. M. Troup, M. H. Chisholm, and M. Extine, *J. Am. Chem. Soc.*, **97**, 1242 (1975).

(53) This problem also has been considered earlier in our group by M. M.-L. Chen, unpublished.

(54) R. Hoffmann, *J. Chem. Phys.*, **39**, 1397 (1963); R. Hoffmann and W. N. Lipscomb, *ibid.*, **36**, 2179, 3489 (1962); **37**, 2872 (1962).

(55) G. Burns, *J. Chem. Phys.*, **41**, 1521 (1964).

(56) E. Clementi and C. Roetti, *At. Data Nucl. Data Tables*, **14**, 179 (1974).

(57) J. W. Richardson, W. C. Nieuwpoort, R. R. Powell and W. F. Edgell, *At. Data Nucl. Data Tables*, **36**, 1057 (1962).

(58) H. Basch and H. B, Gray, *Theor. Chim. Acta*, **4**, 367 (1967).

(59) R. F. Fenske and D. D. Radtke, *Inorg. Chem.*, **7**, 479 (1968).

(60) J. W. Richardson, R. R. Powell, and W. C. Nieuwpoort, *J. Chem. Phys.*, **38**, 796 (1963).

(61) M. Zerner and M. Gouterman, *Theor. Chim. Acta*, **4**, 48 (1948).

(62) (a) D. S. Lichtenberger and R. F. Fenske, *J. Am. Chem. Soc.*, **98**, 50 (1976); (b) M. B. Hall and R. F. Fenske, *Inorg. Chem.*, **11**, 1619 (1972).

(63) T. Albright, personal communication.

(64) J. W. Lauher, M. Elian, R. H. Summerville, and R. Hoffmann, *J. Am. Chem. Soc.*, **98**, 3219 (1976).

(65) D. Thorn, personal communication.

(66) H. Basch, A. Viste, and H. B. Gray, *Theor. Chim. Acta*, **3**, 458 (1965); V. I. Baranovskii and A. B. Nikol'skii, *Teor. Eksp. Khim.*, **3**, 527 (1967).